Respiratory-cardiovascular Interactions During Mechanical Ventilation: Physiology and Clinical Implications

*John Kreit**

ABSTRACT

Positive-pressure inspiration and positive end-expiratory pressure (PEEP) increase pleural, alveolar, lung transmural, and intra-abdominal pressure, which decrease right and left ventricular (RV; LV) preload and LV afterload and increase RV afterload. The magnitude and clinical significance of the resulting changes in ventricular function are determined by the delivered tidal volume, the total level of PEEP, the compliance of the lungs and chest wall, intravascular volume, baseline RV and LV function, and intra-abdominal pressure. In mechanically ventilated patients, the most important, adverse consequences of respiratory-cardiovascular interactions are a PEEP-induced reduction in cardiac output, systemic oxygen delivery, and blood pressure; RV dysfunction in patients with ARDS; and acute hemodynamic collapse in patients with pulmonary hypertension. On the other hand, the hemodynamic changes produced by respiratory-cardiovascular interactions can be beneficial when used to assess volume responsiveness in hypotensive patients and by reducing dyspnea and improving hypoxemia in patients with cardiogenic pulmonary edema. Thus, a thorough understanding of the physiological principles underlying respiratory-cardiovascular interactions is essential if critical care practitioners are to anticipate, recognize, manage, and utilize their hemodynamic effects. © 2022 American Physiological Society. *Compr Physiol* 12:3425-3448, 2022.

Didactic Synopsis

Major teaching points

- Spontaneous and mechanical ventilation cause cyclical changes in pleural (P_{PL}), alveolar (P_{ALV}), lung transmural ($P_{L\text{-}TM}$), and intra-abdominal (P_{AB}) pressure, which alter venous return and right and left ventricular preload and afterload. The resulting hemodynamic changes define the respiratory-cardiovascular interactions.
- During positive-pressure inflation,
  - An increase in P_{PL} decreases right ventricular (RV) preload.
  - A rise in $P_{L\text{-}TM}$ and P_{ALV} increases RV afterload.
  - The increase in P_{PL} decreases left ventricular (LV) afterload.
  - The fall in RV preload and rise in RV afterload reduce RV stroke volume, which decreases LV preload and stroke volume after several cardiac cycles.
- Positive end-expiratory pressure (PEEP) elevates P_{PL}, P_{ALV}, $P_{L\text{-}TM}$, and P_{AB} throughout the respiratory cycle; thus, its hemodynamic effects are usually greater than those produced by intermittent, positive-pressure breaths alone.
- In mechanically ventilated patients, the magnitude and clinical significance of respiratory-cardiovascular interactions depend on the delivered tidal volume, total PEEP, lung and chest wall compliance, intravascular volume, baseline ventricular function, and intra-abdominal pressure.
- In mechanically ventilated patients, adverse consequences of respiratory-cardiovascular interactions include preload-dependent hypotension and acute RV dysfunction, which can progress to hemodynamic collapse.
- The hemodynamic effects of respiratory-cardiovascular interactions can be beneficial when used to assess volume responsiveness in hypotensive patients and to reduce dyspnea and improve hypoxemia in patients with cardiogenic pulmonary edema.

Introduction

The respiratory and cardiovascular systems are functionally linked because they play essential, complimentary roles in delivering oxygen to and removing carbon dioxide from

*Correspondence to kreitjw@upmc.edu

Division of Pulmonary, Allergy, and Critical Care Medicine, University of Pittsburgh School of Medicine, Pittsburgh, PA, USA

Published online, July 2022 (*comprehensivephysiology.com*)

DOI:10.1002/cphy.c210003

the cells of the body. But it is the physical link—the proximity of the heart, great vessels, and lungs within the thorax and the close apposition of alveolar gas and pulmonary capillary blood—that causes ventilation to alter cardiac function and blood flow to and from the heart. These effects are often referred to as *heart-lung interactions*, but this term is misleading because it implies that the heart is acting on the lungs rather than the other way around and that the heart is the only part of the cardiovascular system affected; it also neglects the important role of the chest wall. In this article, the more accurate term *respiratory-cardiovascular interactions* is used.

This article discusses the relevant physiological principles that govern the function of the respiratory and cardiovascular systems, explains how ventilation alters cardiovascular function, and reviews clinically important respiratory-cardiovascular interactions in mechanically ventilated patients. Although the hemodynamic consequences of positive-pressure ventilation are emphasized, the effects of spontaneous ventilation may be inferred from the principles discussed and will be specifically mentioned when appropriate. Respiratory-cardiovascular interactions during spontaneous breathing have been reviewed by others (35, 78, 161). Abbreviations are listed in Table 1.

Table 1 List of Abbreviations

Pressures	
P_{AB}	intra-abdominal pressure
P_{ALV}	alveolar pressure
P_{ATM}	atmospheric pressure
P_{AW}	airway pressure
$P_{C\text{-}I}$	pulmonary capillary inflow pressure
$P_{C\text{-}IM}$	pulmonary capillary intramural pressure
$P_{C\text{-}O}$	pulmonary capillary outflow pressure
$P_{C\text{-}TM}$	pulmonary capillary transmural pressure
$P_{CW\text{-}TM}$	chest wall transmural pressure
PEEP	positive end-expiratory pressure
$PEEP_T$	total positive end-expiratory pressure
P_{EM}	extramural pressure
P_{ER}	total pressure to balance elastic recoil
P_{ES}	esophageal pressure
P_{IM}	intramural pressure
$P_{IVC\text{-}IM}$	inferior vena cava intramural pressure
$P_{IVC\text{-}TM}$	inferior vena cava transmural pressure
$P_{LA\text{-}IM}$	left atrial intramural pressure
$P_{L\text{-}TM}$	lung transmural pressure
P_{MS}	mean systemic filling pressure
P_{PL}	pleural pressure
$P_{RA\text{-}IM}$	right atrial intramural pressure
$P_{RA\text{-}TM}$	right atrial transmural pressure
P_{RES}	total pressure to overcome flow-resistive forces
$P_{RS\text{-}TM}$	respiratory system transmural pressure
$P_{SVC\text{-}IM}$	superior vena cava intramural pressure
$P_{SVC\text{-}TM}$	superior vena cava transmural pressure
P_{TM}	transmural pressure
Volumes and flows	
$\dot{V}$	flow
$\dot{V}_{VR}$	rate of venous return
EV	equilibrium volume
FRC	functional residual capacity
RV	residual volume
TLC	total lung capacity
V	volume
V_T	tidal volume
Compliance, elastance, and resistance	
C	compliance
E	elastance
E_{CW}	chest wall elastance
E_L	lung elastance
E_{RS}	respiratory system elastance
PVR	pulmonary vascular resistance
R	resistance
R_{AW}	airway resistance
R_{RS}	total respiratory system resistance
R_{VR}	resistance to venous return
SVR	systemic vascular resistance

The Respiratory System

The respiratory system is composed of the lungs and the chest wall, which consists of the rib cage, thoracic spine, and all attached soft tissue and muscles, including the diaphragm. The chest wall defines the extent of the thorax, which also contains the heart, superior vena cava, pulmonary circulation, thoracic aorta, and esophagus.

The function of the respiratory system is to optimize *gas exchange*, whereby oxygen (O_2) is added to, and carbon dioxide (CO_2) is removed from the mixed venous blood pumped into the pulmonary circulation by the right ventricle. This requires effective *ventilation*, the cyclical movement of gas into and out of the lungs. Ventilation can occur only when pressure is applied to overcome *elastic and flow-resistive forces*, which oppose changes in lung and chest wall volume and gas flow through the conducting airways. The interaction of these applied and opposing forces is referred to as the mechanics of ventilation or *respiratory mechanics*.

Opposing forces

Elastic forces

The lungs and chest wall are elastic structures. That is, each has a resting or equilibrium volume, and any volume change requires an applied pressure to balance *elastic recoil* generated by elastin, collagen, and alveolar surface tension in the lungs and by cartilage, muscle, connective tissue, and bone in the chest wall. Although the lungs and chest wall act as

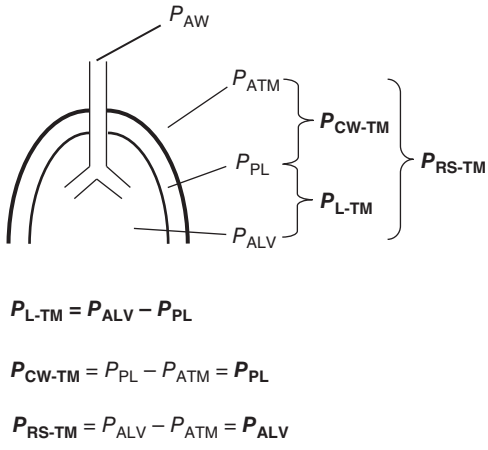

Figure 1 Illustration showing the transmural pressure of the lungs ($P_{L\text{-}TM}$), chest wall ($P_{CW\text{-}TM}$), and respiratory system ($P_{RS\text{-}TM}$). P_{AW}, airway pressure; P_{ALV}, alveolar pressure; P_{PL}, pleural pressure; P_{ATM}, atmospheric pressure. From Kreit J. Mechanical Ventilation. Oxford University Press, 2018. Reproduced with permission of the licensor through PLSclear.

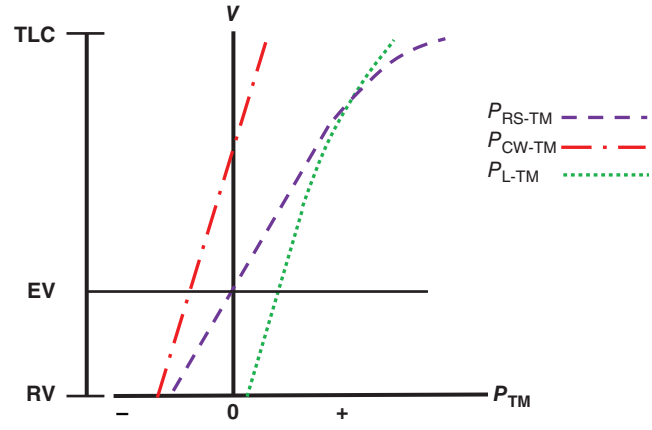

Figure 2 Static expiratory volume-transmural pressure curves of the lungs ($P_{L\text{-}TM}$), chest wall ($P_{CW\text{-}TM}$), and respiratory system ($P_{RS\text{-}TM}$). $P_{CW\text{-}TM}$ equals pleural pressure, $P_{RS\text{-}TM}$ equals alveolar pressure, and $P_{L\text{-}TM}$ equals alveolar pressure minus pleural pressure. V, volume; P_{TM}, transmural pressure; TLC, total lung capacity; EV, equilibrium volume; RV, residual volume; +, positive transmural pressure; –, negative transmural pressure. From Kreit J. Mechanical Ventilation. Oxford University Press, 2018. Modified with permission of the licensor through PLSclear.

a single structure and share a common volume, the elastic properties of each may be determined by measuring changes in lung volume (V) and the accompanying change in *transmural pressure* (P_{TM}) under static (i.e., zero-flow) conditions (1, 108, 116, 126).

Transmural pressure is the gradient across the wall of an elastic structure; it is calculated by subtracting the pressure on the outer surface (extramural pressure; P_{EM}) from the pressure on the inner surface (intramural pressure; P_{IM}).

$$P_{TM} = P_{IM} - P_{EM} \quad (1)$$

As illustrated in Figure 1, lung transmural pressure ($P_{L\text{-}TM}$) is the difference between alveolar pressure (P_{ALV}) and pleural pressure (P_{PL}), and chest wall transmural pressure ($P_{CW\text{-}TM}$) equals P_{PL} minus the pressure at the body surface, which is atmospheric pressure (P_{ATM}). The transmural pressure of the entire respiratory system ($P_{RS\text{-}TM}$) is P_{ALV} minus P_{ATM}.

Static volume-transmural pressure (V-P_{TM}) curves can be constructed by having a subject perform measured, stepwise exhalations from total lung capacity (TLC) to residual volume (RV) (1, 108, 116). At each volume, the airway opening is occluded, and, with the respiratory muscles completely relaxed, the pressure proximal to the occlusion (airway pressure; P_{AW}) and the pressure within the esophagus (P_{ES}) are measured. This allows $P_{L\text{-}TM}$, $P_{CW\text{-}TM}$, and $P_{RS\text{-}TM}$ to be calculated at each volume (Figure 1). Note that (i) P_{ES} is used as a surrogate for P_{PL}; (ii) in the absence of gas flow, P_{AW} is assumed to equal P_{ALV}; and (iii) P_{ATM} is assigned a value of zero because all other pressures are referenced to it.

Normal, expiratory, V-P_{TM} curves are shown in Figure 2; several features deserve emphasis (1, 108, 116). First, as shown in Figure 1, $P_{CW\text{-}TM}$ equals P_{PL}, and $P_{RS\text{-}TM}$ equals P_{ALV}. Second, P_{TM} is synonymous with *elastic recoil pressure*. That is, at each volume, P_{TM} is the pressure generated by the inward or outward recoil of the lungs, chest wall, or respiratory system. It is also the applied pressure needed to balance elastic recoil at each volume. Inward recoil is designated by positive pressures on the X-axis; negative pressures indicate outward recoil. It follows that elastic recoil disappears when P_{TM} is zero. This corresponds to the equilibrium volume of each structure and is the point at which the chest wall and respiratory system curves cross the Y-axis. The equilibrium volume of the lungs is below RV; thus, $P_{L\text{-}TM}$ does not reach zero. Third, at every volume, $P_{RS\text{-}TM}$ (P_{ALV}) is the sum of $P_{L\text{-}TM}$ ($P_{ALV} - P_{PL}$) and $P_{CW\text{-}TM}$ (P_{PL}). Note that the respiratory system reaches its equilibrium volume when $P_{L\text{-}TM}$ and $P_{CW\text{-}TM}$ are equal and opposite, and $P_{RS\text{-}TM}$ is zero. Normally, this is the volume remaining at the end of a passive (i.e., no patient effort) exhalation and is designated the functional residual capacity (FRC).

At every volume, elastic recoil pressure is greater during inspiration than during expiration, a property referred to as *hysteresis* (1, 19, 87, 126). Chest wall hysteresis is produced by connective tissue and muscle, which demonstrate similar properties in vitro. Lung hysteresis is attributed mostly to surfactant, which, at each lung volume, reduces alveolar surface tension more during expiration than during inspiration.

Elastic forces are usually quantified by *compliance* (C), which is the ratio of the simultaneous change in volume (ΔV) and transmural pressure (ΔP_{TM}) under zero-flow conditions (1, 108, 116).

$$C = \Delta V / \Delta P_{TM} \quad (2)$$

Note that compliance varies inversely with elastic recoil. Lung, chest wall, and respiratory system compliance are calculated by substituting the change in $P_{L\text{-}TM}$, $P_{CW\text{-}TM}$,

and $P_{RS\text{-}TM}$, respectively into the denominator of Eq. (2). Compliance is also equal to the slope of the V-P_{TM} curves shown in Figure 2. Rearranging Eq. (2) shows that the elastic recoil pressure (P_{ER}) and the pressure needed to balance it, vary directly with the change in volume and inversely with compliance,

$$P_{ER} = \Delta P_{TM} = \Delta V/C \quad (3)$$

and that the change in volume is determined by the product of compliance and the change in transmural pressure.

$$\Delta V = \Delta P_{TM} \times C \quad (4)$$

Elastic forces may also be quantified by *elastance*, which is the reciprocal of compliance and varies directly with elastic recoil.

Flow-resistive forces

Under static conditions, maintaining the respiratory system at any point above or below its equilibrium volume requires only enough pressure to balance elastic recoil. During the dynamic processes of inspiration and expiration, however, additional pressure must be supplied to overcome *flow-resistive forces* that oppose gas flow and movement of the lungs and chest wall (24–26, 57, 65, 85, 86, 98, 119). This pressure (P_{RES}) generates a gradient between P_{AW} and P_{ALV}, overcomes the friction produced by movement of the lungs and chest wall, and is dissipated by the viscoelasticity of the lung parenchyma and chest wall as the tissues stretch and relax throughout the respiratory cycle (24–26, 65).

The intramural pressure gradient (ΔP_{IM}) between the airway opening and the alveoli is needed to overcome friction at the airway surface and the cohesive forces between gas molecules. It can be thought of both as the driving pressure required to produce flow and as the pressure lost to flow-resistive forces. The magnitude of ΔP_{IM} depends on the rate of gas flow, the length and caliber of the airways, and the density and viscosity of the gas. The relative importance of these factors depends on the characteristics of gas flow (57).

When flow is *laminar*, gas moves in discrete, cylindrical layers or laminae, and ΔP_{IM} is directly proportional to flow ($\dot{V}$), airway length (L), and gas viscosity (η) and inversely related to the fourth power of the airway radius (r).

$$\Delta P_{IM} \propto \dot{V} L\eta/r^4 \quad (5)$$

As gas velocity increases and the airways become more branched and irregular, *turbulent* flow develops as gas movement becomes increasingly chaotic and disorganized. Turbulent flow requires a much higher driving pressure—ΔP_{IM} varies directly with the *square* of the flow rate and inversely with the *fifth* power of the airway radius—and ΔP_{IM} is directly proportional to gas density (ρ) instead of viscosity (57).

$$\Delta P_{IM} \propto \dot{V}^2 L\rho/r^5 \quad (6)$$

Since flow through the conducting airways has both laminar and turbulent components, Eqs. (5) and (6) are often combined into a single equation that incorporates airway length and radius and gas viscosity or density into the constants K_1 and K_2.

$$\Delta P_{IM} \propto K_1 \dot{V} + K_2 \dot{V}^2 \quad (7)$$

When flow is predominantly laminar, the first term predominates, and the relationship between driving pressure and flow is nearly linear. As flow becomes more turbulent, the second term assumes increasing importance, and pressure losses increase exponentially with flow (57).

Whereas compliance and elastance are used to quantify elastic recoil, flow-resistive forces are expressed in terms of *resistance* (R), which is the ratio of P_{RES} (or its airway, frictional, or viscoelastic component) and gas flow (24–26, 65). Thus, total respiratory system resistance (R_{RS}) is

$$R_{RS} = P_{RES}/\dot{V} \quad (8)$$

and the total pressure needed to overcome flow-resistive forces equals the product of flow and respiratory system resistance.

$$P_{RES} = \dot{V} \times R_{RS} \quad (9)$$

Airway resistance (R_{AW}) equals the pressure gradient between the airway opening and the alveoli divided by flow.

$$R_{AW} = \Delta P_{IM}/\dot{V} = (P_{AW} - P_{ALV})/\dot{V} \quad (10)$$

Substituting Eqs. (5) and (6) into Eq. (7) and dividing both sides by flow yields

$$R_{AW} \propto L\eta/r^4 + \dot{V} L\rho/r^5 \quad (11)$$

Thus, airway radius is the most important determinant of R_{AW}, and when flow is turbulent, R_{AW} increases in proportion to the flow rate. Rearranging Eq. (10) shows that flow is directly proportional to ΔP_{IM} and inversely related to airway resistance.

$$\dot{V} = (P_{AW} - P_{ALV})/R_{AW} \quad (12)$$

Applied forces

The equation of motion

Equations (3) and (9) define the pressure needed to overcome elastic and flow-resistive forces, respectively. Thus, the total pressure (P_{TOT}) supplied by the respiratory muscles, a mechanical ventilator, or both at any point during inspiration is defined by the *equation of motion* as the sum of P_{ER} and P_{RES} (57).

$$P_{TOT} = P_{ER} + P_{RES} = \Delta V/C + (\dot{V} \times R_{RS}) \quad (13)$$

During mechanical ventilation, the total positive end-expiratory pressure ($PEEP_T$) must be added.

$$P_{TOT} = \Delta V/C + (\dot{V} \times R_{RS}) + PEEP_T \quad (14)$$

Spontaneous ventilation

The diaphragm normally supplies most of the pressure required for spontaneous tidal inspiration (30, 32). As it contracts, the diaphragm flattens and moves downward like a piston while simultaneously forcing the rib cage outward. This increases the volume of the thorax and lungs and decreases the volume of the abdominal compartment, which raises intra-abdominal pressure (P_{AB}). Expiration, when passive, is driven solely by the stored elastic recoil of the respiratory system.

Figure 3 illustrates the change in P_{PL}, P_{ALV}, $P_{L\text{-}TM}$, and P_{AB} during a spontaneous breath (85, 86, 98, 119). Note that these are *dynamic*, pressure-time curves, as opposed to the static V-P_{TM} curves shown in Figure 2. Airway pressure (not shown) always equals P_{ATM}. At end-expiration, the elastic recoil of the lungs and chest wall pulls the visceral and parietal pleura in opposite directions, which makes mean P_{PL} negative relative to P_{ATM}. During inspiration, inward lung recoil increases as the lungs are pulled outward by the expanding chest wall; thus, P_{PL} decreases and reaches its most negative value at end-inspiration. Throughout passive expiration, lung elastic recoil decreases, and P_{PL} returns to its baseline value. When gas flow stops at end-expiration, P_{ALV} equals P_{AW} and P_{ATM} (0 cmH_2O). When inspiration begins, lung volume increases faster than gas enters, and P_{ALV} falls; this produces the pressure gradient ($P_{AW} - P_{ALV}$) that drives gas through the conducting airways. As the lungs fill, P_{ALV} increases until it returns to zero (and flow stops) at end-inspiration. The opposite occurs during passive exhalation, and P_{ALV} returns to zero when flow stops at end-expiration (85, 86, 98, 119). Lung transmural pressure and P_{AB} are positive (supra-atmospheric) at end-expiration and increase and decrease with lung volume throughout the respiratory cycle.

Mechanical ventilation

Dynamic pressure-time curves during a passive mechanical breath are shown in Figure 4. Unlike spontaneous breaths, P_{AW} and P_{ALV} increase during positive-pressure inflation. The rising P_{ALV} balances the increasing elastic recoil of the respiratory system, and the gradient between P_{AW} and P_{ALV} overcomes flow-resistive forces and drives gas through the conducting airways. If an end-inspiratory pause is performed, flow stops, the delivered volume is held in the lungs, flow-resistive forces disappear, and P_{AW} falls to P_{ALV}. Lung inflation pushes the visceral pleura against the parietal pleura of the chest wall, and mean P_{PL} rises. The difference between P_{ALV} and P_{PL} ($P_{L\text{-}TM}$) also increases with lung volume. By expanding the lungs, mechanical inflation forces

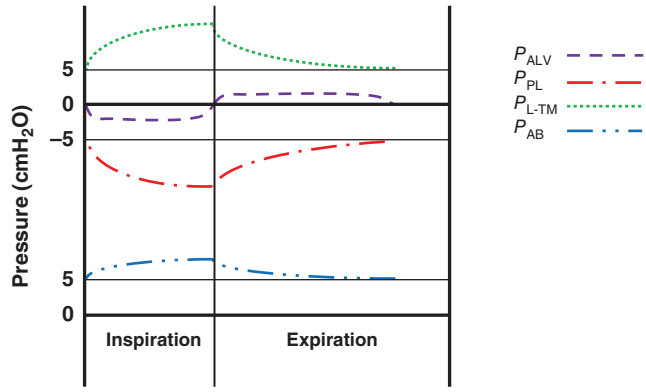

Figure 3 Dynamic pressure-time curves showing the change in alveolar (P_{ALV}), pleural (P_{PL}), lung transmural ($P_{L\text{-}TM}$), and intra-abdominal (P_{AB}) pressure during a spontaneous breath. Based on, with permission, Mead J and Whittenberger JL, 1953 (86); Mead J, 1961 (85); Otis AB, et al., 1950 (98); Rodarte JR and Rehder K, 2011 (119).

the diaphragm downward, thereby increasing P_{AB}. During passive expiration, P_{AW}, P_{ALV}, P_{PL}, $P_{L\text{-}TM}$, and P_{AB} return to baseline, and flow stops when P_{ALV} equals P_{AW}.

When added by the clinician during mechanical ventilation, PEEP is the pressure in cmH_2O by which end-expiratory P_{AW} and P_{ALV} are raised above P_{ATM} (Figure 4B). This stops expiratory flow prematurely, increases end-expiratory lung volume by the product of applied PEEP ($\Delta P_{RS\text{-}TM}$) and respiratory system compliance (Eq. 4), and produces a new, higher equilibrium volume.

End-expiratory volume and P_{ALV} also increase when expiratory time is insufficient to allow the respiratory system to return to its normal equilibrium volume; this is called *dynamic hyperinflation*. It occurs when the time available for expiration is very short or, more commonly, when the time required for complete tidal expiration is prolonged by reduced respiratory system elastic recoil (high compliance), high airway resistance, or both. In clinical practice, dynamic hyperinflation most often occurs in patients with moderate to severe obstructive lung disease. In patients with dynamic hyperinflation, the level of end-expiratory P_{ALV} is called "intrinsic" PEEP to distinguish it from clinician-added, "extrinsic" PEEP. Both extrinsic and intrinsic PEEP cause a proportional rise in P_{ALV}, P_{PL}, $P_{L\text{-}TM}$, and P_{AB} throughout the respiratory cycle.

The Cardiovascular System

The cardiovascular system consists of the heart and two distinct circulations. The right ventricle (RV) ejects the mixed, systemic venous blood into the pulmonary circulation, where pulmonary gas exchange occurs. The left ventricle (LV) pumps the mixed, pulmonary venous blood into the systemic circulation, where tissue gas exchange provides O_2 to and removes CO_2 from the cells of the body.

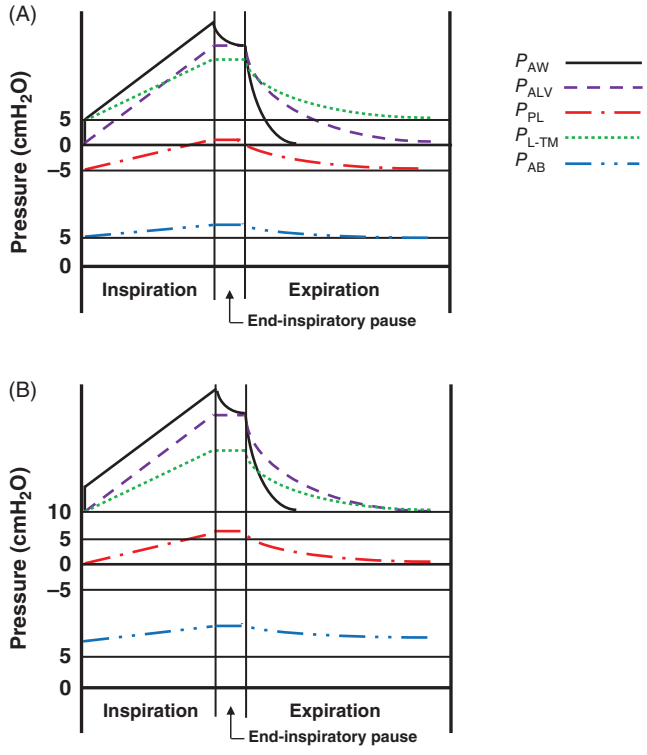

Figure 4 Dynamic pressure-time curves during a passive, mechanical breath with constant inspiratory flow and positive end-expiratory pressure (PEEP) of 0 cmH_2O (A) and 10 cmH_2O (B). PEEP causes a proportional rise in airway (P_{AW}), alveolar (P_{ALV}), pleural (P_{PL}), lung transmural ($P_{L\text{-}TM}$), and intra-abdominal (P_{AB}) pressure throughout the respiratory cycle. When inspiratory flow stops and expiration is delayed by an end-inspiratory pause, P_{AW} falls to P_{ALV}. Based on, with permission, Van den Berg PCM, et al., 2002 (142).

Like the lungs and chest wall, the heart chambers and blood vessels are elastic structures, and like gas flow through the conducting airways, blood flow requires an intramural pressure gradient. Thus, any change in atrial, ventricular, or vascular volume is determined by the product of compliance and ΔP_{TM} (Eq. 4); the required ΔP_{IM} depends on the length and caliber of the blood vessels, blood viscosity and density, the rate of blood flow, and whether flow is mostly laminar or turbulent (Eqs. 5-7); and vessel radius is the most important determinant of vascular resistance (Eq. 11).

The systemic and pulmonary circulations have many important differences that influence the effect and magnitude of respiratory-cardiovascular interactions (139, 153, 154). The systemic arteries are highly muscularized with thick walls and relatively small lumens; thus, arterial compliance is low, systemic vascular resistance is high, and a large pressure gradient is needed to drive blood flow. In comparison, the thin media of the pulmonary arteries contains multiple elastic laminae and relatively little smooth muscle; thus, the normal pulmonary circulation has high compliance and low resistance. This has two important effects: (i) relatively little pressure is needed to pump the systemic venous return from the RV to the left atrium and (ii) vascular caliber and resistance are strongly influenced by intramural and extramural pressure. Thus, the intra-parenchymal vessels dilate during lung inflation, and the pulmonary arteries passively distend during RV ejection then recoil, allowing blood flow to continue during diastole.

Right and left ventricular structure and function are tailored to meet the requirements imposed by their respective circulations (31, 121). The LV has thick walls that can generate the high pressures needed to force blood through the systemic circulation. In contrast, the RV, which must generate only a small fraction of this pressure, has a much thinner free wall, and its mass is normally about one-sixth that of the LV (121).

The cardiac cycle

The process by which the ventricles deliver pulsatile blood flow to the pulmonary and systemic circulations can be divided into four phases based on ventricular pressure and volume—two during systole and two during diastole. These phases are illustrated by ventricular *pressure-volume (P-V) loops* (93, 132). As shown in Figure 5, the normal LV generates a nearly rectangular loop. In contrast, the normal RV *P-V* relationship reaches a much lower pressure and has a trapezoidal or triangular shape. The volume difference between vertical segments of the *P-V* loop is the stroke volume, and the area within the loop equals the work done by the ventricle during systole (the stroke work); this is proportional to myocardial O_2 consumption (93, 132).

- Systole—Isovolumic contraction: At the onset of systole, the ventricles contain the *end-diastolic volume*. Immediately after contraction begins, ventricular P_{IM} exceeds the pressure within the atrium, and the tricuspid and mitral valves close. Because the pulmonic and aortic valves are also closed, the myocardium contracts isometrically, and ventricular pressure rapidly increases without a change in blood volume. This phase ends when RV and LV pressure exceed pulmonary artery diastolic and aortic diastolic pressure, respectively.
- Systole—Ejection: During this phase, the pulmonic and aortic valves open and the ventricles eject the stroke volume. Right ventricular pressure peaks early during ejection, whereas LV pressure rises and falls more gradually. The pulmonic and aortic valves close once RV and LV pressure fall below the pressure within their respective circulations, and systole ends. This corresponds to the pressure at the dicrotic notch in the pulmonary artery and aortic pressure waveforms.
- Diastole—Isovolumic relaxation: With all four valves closed, the blood volume remaining in the ventricles (the *end-systolic volume*) is constant as myocardial tension and ventricular pressure rapidly fall. Despite its name, myocardial relaxation is an energy-dependent process produced by the movement of calcium back into the sarcoplasmic reticulum; thus, it is often referred to as

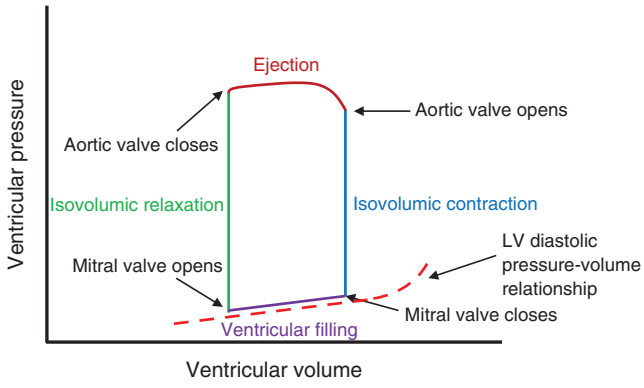

Figure 5 Schematic illustration of the left ventricular (LV) pressure-volume loop. The pressure and volume changes during isovolumic contraction, ejection, isovolumic relaxation, and ventricular filling are shown. The base of the loop is the LV diastolic pressure-volume relationship.

"active relaxation." This phase ends when intraventricular pressure falls below atrial P_{IM} and the tricuspid and mitral valves open.

- Diastole—Ventricular filling: Throughout systole and isovolumic relaxation, the atria fill with blood, and pressure rises. With the opening of the tricuspid and mitral valves, blood rapidly enters the ventricles at a rate proportional to the atrial-ventricular pressure difference. This "passive filling" ends when atrial and ventricular pressures equilibrate. Just before the end of diastole, "active filling" occurs as atrial contraction pushes the final portion of what will become the end-diastolic volume into the ventricle. The ventricular filling phase ends at the onset of systole when the rapid reversal of the atrial-ventricular pressure gradient and contraction of the papillary muscles close the tricuspid and mitral valves.

The determinants of ventricular function

Preload

In 1914, Ernest Starling and colleagues published a series of papers describing the results of experiments performed in an isolated dog heart preparation (83, 101, 102). By measuring cardiac output and right and left atrial pressure while independently varying arterial resistance and pressure and the rate at which venous blood returned to the right atrium, these experiments identified or confirmed many basic principles of cardiovascular physiology. The most well-known findings (101), however, came from building on the work of Otto Frank who, in the late 19th century, described the relationship between LV diastolic volume and force generation in the frog heart (42).

Starling showed that within the normal working range of the ventricle, the tension and pressure generated by the myocardium during systole was directly related to the "load" placed on it by the end-diastolic volume and thus proportional to the length of the myocardial "muscle fibers" prior to contraction (101). This came to be known as the "Frank-Starling mechanism" and the "Frank-Starling law of the heart." By 1914, this "law" had already been well established for skeletal muscle (14).

Subsequently, the term "preload" was adopted to describe the ventricular end-diastolic pressure; that is, the pressure just *before* the onset of contraction. Investigators also used experimental data from intact animal models to construct *ventricular function* or *Starling curves* for both the RV and LV by plotting stroke volume or stroke work on the *Y*-axis and the appropriate mean atrial pressure, as a surrogate for ventricular end-diastolic pressure, on the *X*-axis (11, 12, 122). With advancements in technology, it was recognized that muscle fiber length reflected the length of the sarcomeres, the fundamental contractile units within the cardiac myocytes (54, 71, 133). At the same time, improvements in cardiac catheterization and echocardiography allowed much more accurate measurements of ventricular end-diastolic pressure and volume.

Although preload is typically equated with end-diastolic pressure, its relationship to end-diastolic volume and sarcomere length depends on ventricular diastolic compliance. In the healthy heart, ventricular filling occurs with little increase in intramural or transmural pressure (Figure 6 and the diastolic *P-V* relationship in Figure 5), and end-diastolic pressure is low. When heart disease reduces compliance, ventricular pressure increases more rapidly, the diastolic *P-V* relationship is shifted upward and to the left, and ventricular filling is reduced at the same end-diastolic pressure. When diastolic compliance is abnormally high, as in the failing, dilated heart, the diastolic *P-V* relationship is shifted downward and to the right, and diastolic volume is increased at a given ventricular pressure. Even in the normal heart, however, compliance falls rapidly at high diastolic volumes as the ventricle reaches the limit of its distensibility. Thus, ventricular pressure rapidly increases with little or no increase in ventricular volume (and sarcomere length).

The shape of the normal ventricular function curve can be predicted based on the diastolic *P-V* relationship (Figure 7). Within the optimal working range of the ventricles, stroke volume rapidly increases with end-diastolic volume, which generates only a small increase in end-diastolic pressure. Thus, the curve is initially steep and almost linear. At high end-diastolic volumes, however, ventricular end-diastolic pressure rapidly increases with little or no change in end-diastolic volume and stroke volume, and the curve abruptly plateaus. This means that even small changes in preload can have a significant effect on stroke volume when end-diastolic volume and pressure are normal or low. Once the plateau of the curve is reached, however, further increases in preload raise ventricular wall stress (see next section) but no longer augment ventricular output.

Because they are connected in series, the preload of both ventricles is regulated primarily by the rate at which

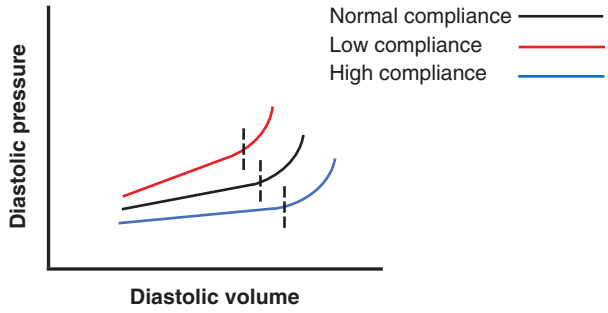

Figure 6 The relationship between diastolic pressure and volume when ventricular compliance is normal, decreased, and increased. As compliance falls, end-diastolic volume decreases at a given end-diastolic pressure, and a higher end-diastolic pressure is required for a given end-diastolic volume. Note that compliance rapidly falls when end-diastolic volume exceeds the normal working range of the ventricle (dashed black lines), and there is little or no increase in ventricular volume as pressure rises. This creates the plateau on the ventricular function curve.

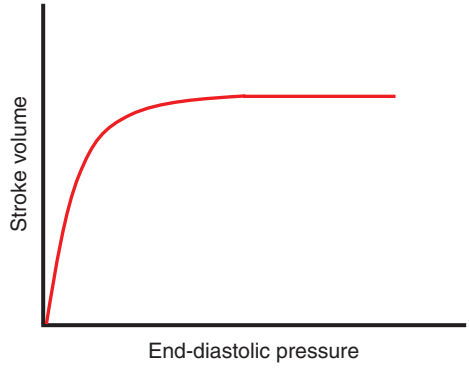

Figure 7 Idealized depiction of a ventricular function or Starling curve. Within the optimal working range of the ventricle, stroke volume increases rapidly with end-diastolic volume with little increase in end-diastolic pressure. At high end-diastolic volumes, however, ventricular compliance rapidly falls, and end-diastolic pressure increases with little or no change in end-diastolic volume and stroke volume.

systemic venous blood returns to the right atrium (RA). The determinants of venous return were defined by a series of experiments performed in the 1950s by Guyton and colleagues (47–50). Guyton's experiments used an open-chest canine preparation in which blood was pumped from the RA, through an external circuit, and into the main pulmonary artery, thereby bypassing the RV. Guyton varied right atrial intramural pressure ($P_{RA\text{-}IM}$), measured the resulting blood flow through the external circuit (venous return), and used this paired data to construct *venous return curves* (47–50). These curves have since been reproduced in intact animal preparations by several investigators (40, 111). As shown in Figure 8, venous return is inversely related to $P_{RA\text{-}IM}$ and stops once $P_{RA\text{-}IM}$ reaches the pressure at the *X*-intercept. This is called the *mean systemic filling pressure* (P_{MS}) and is the "upstream" pressure pushing blood toward the heart. It is generated by the interaction of the veins and venules with the "stressed volume" of the circulating blood and is determined

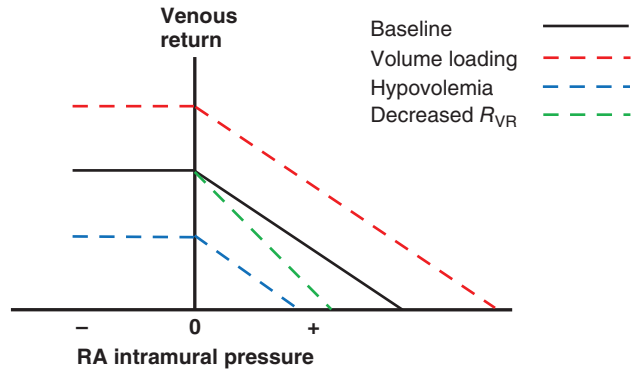

Figure 8 Venous return curves. Mean systemic filling pressure is the point at which each curve intersects the *X*-axis. The effect of volume loading, hypovolemia, and decreased resistance to venous return (R_{VR}) is shown. RA, right atrial; R_{VR}, resistance to venous return; +, positive pressure; –, negative pressure. Based on, with permission, Guyton AC, et al., 1959 (47); Guyton AC, et al., 1956 (49); Guyton AC, et al., 1957 (50); Guyton AC, 1955 (47).

by intravascular volume, venous elastic recoil and autonomic tone, and the extramural pressure acting on these vessels. In animal (51, 111) and human (64, 118) studies, P_{MS} has been equated with $P_{RA\text{-}IM}$ during cardiac arrest. In humans, P_{MS} is approximately 10 mmHg (64, 118).

Thus, in Guyton's model of the systemic circulation, $P_{RA\text{-}IM}$ acts as the *back pressure* for blood returning to the heart, and the rate of venous return ($\dot{V}_{VR}$) is directly proportional to the $P_{MS} - P_{RA\text{-}IM}$ gradient (the driving pressure) and inversely related to what Guyton called the *resistance to venous return* (R_{VR}) (47–50).

$$\dot{V}_{VR} = (P_{MS} - P_{RA-IM})/R_{VR} \quad (15)$$

This is analogous to Eq. (12), which defines flow through the conducting airways.

Note in Figure 8, however, that venous return does not increase indefinitely. The veins entering the thorax are exposed to atmospheric pressure. Thus, once $P_{RA\text{-}IM}$ drops below P_{ATM}, venous P_{TM} becomes negative, the vessels flutter between opening and closing, and venous return plateaus. This is referred to as *flow limitation* and will be discussed in later sections.

Figure 8 also illustrates two other important physiological principles (47–50). First, hypovolemia reduces venous return by decreasing P_{MS} and the $P_{MS} - P_{RA\text{-}IM}$ gradient while volume loading has the opposite effect. Second, the slope of the venous return curve equals the venous conductance; thus, an increase or decrease in slope indicates a fall or a rise in R_{VR}, respectively.

The heart cannot pump more blood than it receives; thus, in a steady state, cardiac output must equal venous return. Guyton illustrated this principle by superimposing canine venous return and ventricular function curves with $P_{RA\text{-}IM}$ on the *X*-axis and venous return and cardiac output on the *Y*-axis (Figure 9) (47). The ventricular function curve starts to the left of the zero line because intramural, not transmural RA

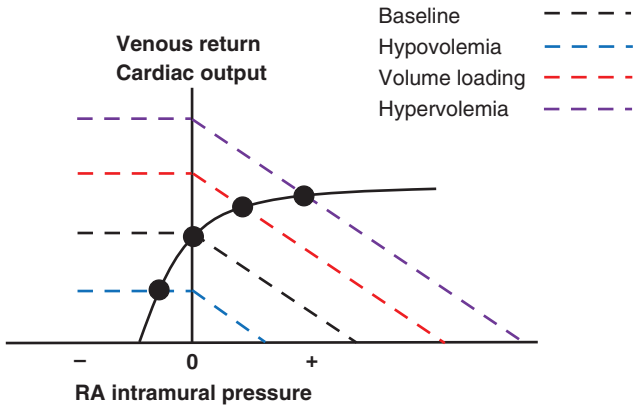

Figure 9 Superimposition of venous return and ventricular function (Starling) curves. Venous return curves over a wide range of intravascular volume and mean systemic filling pressures are shown. Each intersection of a venous return curve with the ventricular function curve (filled circles) defines the right atrial intramural pressure, venous return, and cardiac output at that level of mean systemic filling pressure and ventricular function. RA, right atrial; +, positive pressure; −, negative pressure.

pressure, is being measured. Guyton then showed that for a given P_{MS} and level of ventricular function, $P_{RA\text{-}IM}$, venous return, and cardiac output were determined by the intersection of the two curves. Figure 9 shows that when the ventricle is functioning on the steep portion of its Starling curve, raising the P_{MS} by expanding vascular volume progressively increases venous return and cardiac output with only a small increase in $P_{RA\text{-}IM}$. When the ventricle is functioning on the plateau of its curve, however, raising P_{MS} causes a large increase in $P_{RA\text{-}IM}$ but has no effect on venous return and cardiac output.

Afterload

This is the load that the ventricle must overcome *after* contraction begins. Ventricular afterload is most often equated with the wall stress (σ) developed during the isovolumic phase of systole (132). Although it is a marked over-simplification, circumferential wall stress is usually estimated based on the law of LaPlace for a cylinder (132, 155). Thus, wall stress is directly proportional to ventricular P_{TM} and the internal radius (r) of the ventricular cavity and inversely related to ventricular wall thickness (T) at the end of isovolumic contraction; that is, just prior to the ejection phase of systole (132).

$$\sigma \propto (P_{TM} \times r)/T \quad (16)$$

This equation has several important implications. First, because ventricular internal radius is proportional to end-diastolic volume, afterload increases with ventricular preload. Second, ventricular hypertrophy reduces afterload by distributing wall stress throughout a greater myocardial volume. Finally, because P_{TM} in Eq. (16) is the pressure needed to open the pulmonic and aortic valves, RV and LV P_{TM} can usually be approximated by end-expiratory, intramural pulmonary artery diastolic, and aortic diastolic pressure, respectively. In clinical practice, these pressures are often used as surrogates for RV and LV afterload.

In the absence of outflow obstruction, ventricular afterload has two major determinants (21, 139, 153, 154). The first is pulmonary vascular resistance (PVR) or systemic vascular resistance (SVR); as resistance rises, so does the pressure needed to pump blood through the circulation. Second, afterload increases with the "downstream" or back pressure the ventricle must eject against (139, 153). For the LV, this is the critical closing pressure within the arterial circulation (76); for the RV, the back pressure varies between P_{ALV} and the pressure within the left atrium (LA; $P_{LA\text{-}IM}$), depending on the distribution of pulmonary capillary transmural pressures (see later section: Alveolar and extra-alveolar vessels). Left ventricular afterload is normally high because the LV ejects into the high-resistance systemic circulation; RV afterload is normally low (139, 153).

Contractility

Ventricular contractility is defined as the inherent inotropic state of the myocardium. Neither stoke volume nor stroke work reliably reflect contractility because both are heavily influenced by preload and afterload. Thus, the most accurate assessment of contractility is derived from a series of *P-V* loops plotted under varying load conditions (Figure 10). At a constant heart rate, with either varying preload and constant afterload or varying afterload with constant preload, contractility is proportional to the slope of a line connecting the end-systolic ratio of ventricular pressure to ventricular volume within each loop (132, 155).

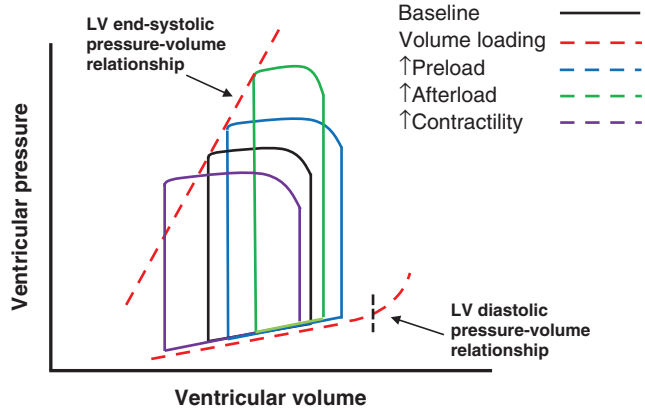

Figure 10 A schematic illustration of the change in the baseline left ventricular (LV) pressure-volume loop (black) with an increase in preload, afterload, and contractility. The slope of a line connecting the end-systolic pressure and volume of loops obtained with different preload and afterload is proportional to ventricular contractility. The LV diastolic pressure-volume relationship and the point at which diastolic compliance rapidly falls (dashed black line) are also shown. Figure modified, with permission, from Tanai E and Frantz S, 2016 (136).

Combining the determinants of ventricular function

Stroke volume is determined by the combined effects of ventricular preload, afterload, and contractility. The interaction and net effect of these three factors can be illustrated by the series of *P-V* loops shown in Figure 10 (122, 132, 136). An increase in preload produced, for example, by an intravenous crystalloid bolus, raises end-diastolic pressure and volume along the diastolic *P-V* curve and increases stroke volume and stroke work. An increase in afterload also shifts the loop along its diastolic *P-V* curve (thereby increasing preload), but stroke volume falls despite higher ventricular pressure. In the normal heart, the rise in preload restores baseline stroke volume after several cardiac cycles but at the expense of an increase in stroke work and O_2 consumption. Finally, an increase in contractility, by raising the peak pressure-volume ratio, widens the *P-V* loop and shifts it to the left on the diastolic *P-V* curve. Thus, stroke volume increases at a lower ventricular preload.

Similar information is provided by the series of Starling curves shown in Figure 11 (122, 132, 136). An increase or decrease in preload moves ventricular function to the right and left, respectively along the same curve. An increase in afterload or a decrease in contractility shifts the curve downward and to the right, thereby reducing stroke volume at a higher preload. An increase in contractility or a decrease in afterload moves the curve upward and to the left, and stroke volume increases at a lower preload.

Ventricular interdependence

The RV and LV share a common septum and are surrounded by the pericardium, which initially stretches but then rapidly stiffens with increasing volume. Thus, total ventricular volume is constrained, and during diastole, an increase in the volume of one ventricle reduces the volume and compliance of the other (137, 160). This is referred to as *diastolic ventricular interdependence*. Although its effects on the healthy heart are small, and under steady-state conditions, RV and LV output must be equal, ventricular interdependence and its hemodynamic consequences can become markedly exaggerated by ventricular dilation and diseases of the pericardium (92, 160).

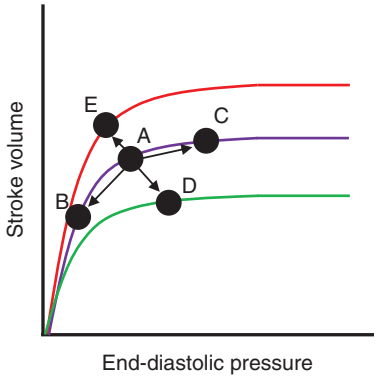

Figure 11 A series of Starling curves showing the effect of changes in ventricular preload, afterload, and contractility. Increases and decreases in preload move ventricular function to the right (A → C) and left (A → B), respectively along the same curve. Increased contractility or decreased afterload move ventricular function upward and to the left (A → E), thereby increasing stroke volume at a lower preload. Increased afterload or decreased contractility move the curve down and to the right, and stroke volume falls at a higher preload (A → D). From Kreit J. Mechanical Ventilation. Oxford University Press, 2018. Reproduced with permission of the licensor through PLSclear.

Extramural pressure and the compartments of the cardiovascular system

Much of the cardiovascular system is exposed to nonatmospheric pressure. Figure 12 shows the "compartments" of the cardiovascular system based on the prevailing extramural pressure (36). Within the thorax, the visceral pleura surrounds both lungs, and the parietal pleura lines the rib cage, diaphragm, and mediastinum. Thus, the heart, superior vena cava (SVC), and pulmonary arteries and veins are exposed to P_{PL}; the pulmonary capillaries, which run through the alveolar walls, are acted on by P_{ALV}; and the intra-abdominal arteries and veins, including the inferior vena cava (IVC), are surrounded by P_{AB}. This is important because these extramural pressures are altered by spontaneous and mechanical ventilation, and changes in P_{EM} affect P_{IM} and P_{TM}, which determine blood flow and blood volume, respectively.

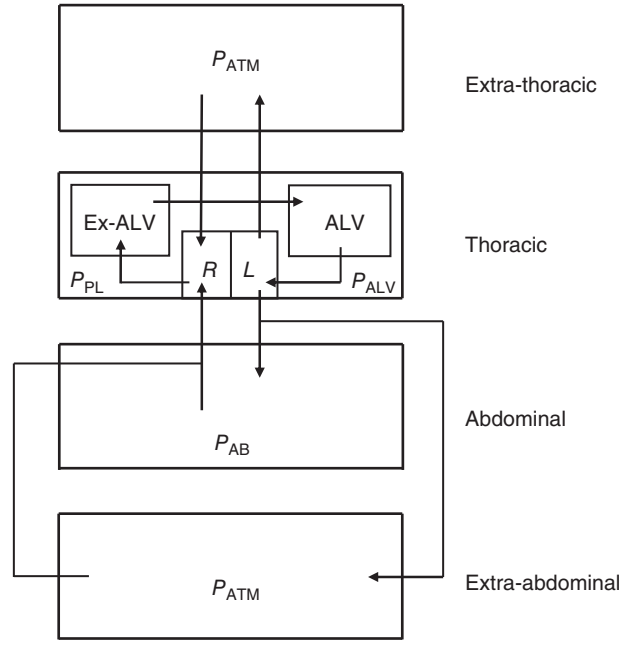

Figure 12 The "compartments" of the cardiovascular system. The extra-thoracic compartment contains the blood vessels in the head, neck, arms, and extra-pleural chest wall. The extra-abdominal compartment consists of the lower body and the extra-peritoneal abdominal wall. P_{ATM}, atmospheric pressure; P_{PL}, pleural pressure; P_{ALV}, alveolar pressure; P_{AB}, intra-abdominal pressure; ALV, alveolar vessels; Ex-ALV, extra-alveolar vessels; R, right atrium and ventricle; L, left atrium and ventricle. From Kreit J. Mechanical Ventilation. Oxford University Press, 2018. Reproduced with permission of the licensor through PLSclear.

The effects of increasing extramural pressure

When the volume and compliance of an elastic structure do not change, P_{TM} must be constant; thus, a change in P_{EM} produces an identical change in P_{IM}. This, for example, allows a balloon catheter to accurately reflect pressure changes within the esophagus or the bladder. The effect of altering the P_{EM} acting on the heart chambers and blood vessels is more complex because volume and P_{TM} usually do change.

The right atrium, superior vena cava, and inferior vena cava

Based on data derived from animal and human studies (72, 112, 134, 135, 142, 145, 147), Figure 13 shows how pressure, blood flow, and volume change during a passive mechanical breath or with PEEP. In the figure, a continuous process has been divided into several steps.

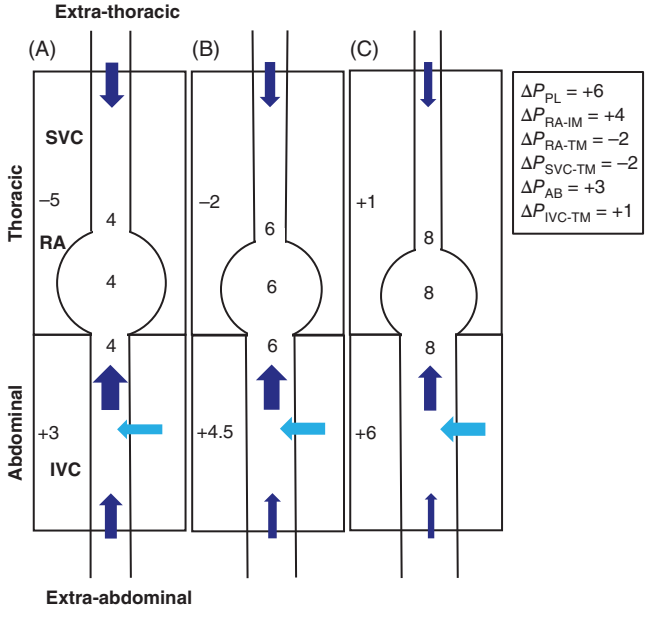

Figure 13 Schematic representation of the right atrium (RA) and superior vena cava (SVC) within the thoracic compartment and the inferior vena cava (IVC) within the abdominal compartment. The figure shows the change in pressure within the RA (P_{RA-IM}), SVC (P_{SVC-IM}), abdomen (P_{AB}), and IVC (P_{IVC-IM}) when pleural pressure (P_{PL}) is increased by a positive-pressure breath or positive end-expiratory pressure. For the sake of clarity, a rapid, continuous process has been separated into three steps (A, B, and C). The total change in P_{PL}, P_{RA-IM}, P_{AB}, and transmural RA (P_{RA-TM}), SVC (P_{SVC-TM}), and IVC (P_{IVC-TM}) pressure is shown in the box. The width of the arrows indicates the magnitude of flow. The size of the RA, SVC, and IVC reflect transmural pressure and volume. Purple arrows represent flow from the extra-thoracic, abdominal, and extra-abdominal compartments. Light blue arrows represent flow from the splanchnic venous reservoir. Based on, with permission, Jellinek H, et al., 2000 (64); Lansdorp B, et al., 2014 (72); Pinsky M, 1984 (111); Pinsky MR, 1984 (112); Takata M, Beloucif S, Shimada M, Robotham JL. Superior and inferior vena caval flows during respiration: pathogenesis of Kussmaul's sign. Am J Physiol 262: H763-H770, 1992; Takata M and Robotham JL, 1990 (134); Takata M, et al., 1992 (135); Van den Berg PCM, et al., 2002 (142); Vieillard-Baron, A, et al., 2001 (151); 137. Vieillard-Baron A, et al., 2004 (147).

With the application of positive airway pressure, the rise in P_{PL} (Figure 4) increases P_{RA-IM} and the pressure within the SVC (P_{SVC-IM}). This is accompanied by a fall in venous return from the extra-thoracic and abdominal compartments. The resulting decrease in RA and SVC volume causes a proportional drop in RA and SVC transmural pressure (P_{RA-TM}; P_{SVC-TM}), which reduces the rate at which P_{RA-IM} and P_{SVC-IM} rise and the rate at which flow and volume fall, and new equilibrium values are reached. Thus, an increase in P_{PL} raises P_{RA-IM} and P_{SVC-IM} and reduces venous return, P_{RA-TM}, P_{SVC-TM}, RA and SVC volume, and SVC diameter.

Simultaneously, diaphragm descent compresses the liver, reduces the volume of the abdominal compartment, and increases P_{AB}, which reduces blood flow from the extra-abdominal compartment. The abdomen, however, contains a large reservoir of venous blood within the splanchnic circulation. If the pressure within the IVC (P_{IVC-IM}) uniformly exceeds P_{AB}, the increase in P_{AB} pushes this blood toward the RA (see later section: Right ventricular preload). Because P_{RA-IM} normally rises more than P_{AB} (142) and is usually the major determinant of upstream P_{IVC-IM}, IVC transmural pressure (P_{IVC-TM}), volume, and diameter increase with positive-pressure inflation and PEEP.

The left atrium, ventricles, and main pulmonary arteries and veins

The rise in P_{PL} with positive-pressure inflation and PEEP also increases the pressure within the LA, RV, and main (mediastinal) pulmonary arteries and veins. However, because these structures are all exposed to P_{PL}, there is no direct effect on driving pressure, blood flow, and volume. Elevation of LV intramural pressure reduces the pressure needed to eject blood from the thorax (see later section: Left ventricular preload and afterload).

Alveolar and extra-alveolar vessels

Based on the compartment model shown in Figure 12, the intra-parenchymal pulmonary circulation can be divided into *alveolar vessels*, which are mostly the pulmonary capillaries, and *extra-alveolar vessels*, which are the pulmonary arteries and veins (23, 56, 107). Because they have no structural rigidity, the caliber of the pulmonary capillaries is determined solely by transmural pressure (P_{C-TM}), which is the difference between the pressure within the capillaries (P_{C-IM}) and P_{ALV}.

At the level of the main pulmonary arteries, P_{C-IM} entering the alveoli (inflow pressure; P_{C-I}) is mean pulmonary arterial pressure minus the pressure lost to flow-resistive forces. At the level of the LA, P_{C-IM} leaving the alveoli (outflow pressure; P_{C-O}) is normally slightly higher than P_{LA-IM}. Gravity-induced changes in hydrostatic pressure cause P_{C-I} and P_{C-O} to increase and decrease by 1.0 cmH_2O, respectively for every centimeter that the vessel is below or above the main pulmonary arteries and LA. Since P_{ALV} can be considered

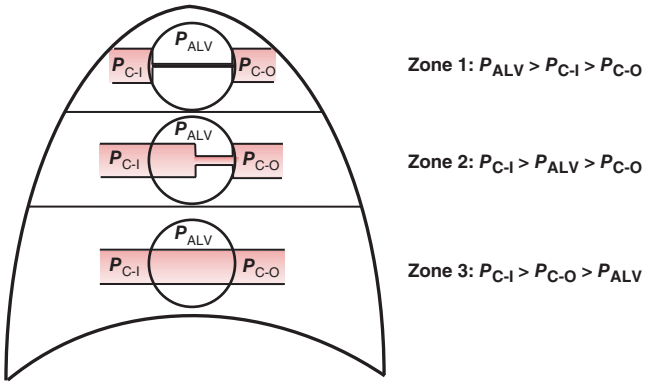

Figure 14 The zones of the lung. P_{ALV}, alveolar pressure; P_{C-I}, capillary inflow pressure; P_{C-O}, capillary outflow pressure. From Kreit J. Mechanical Ventilation. Oxford University Press, 2018. Reproduced with permission of the licensor through PLSclear.

uniform throughout the lungs, P_{C-TM} must vary with the location of the vessel. This is the basis for the *zones of the lung* as described by West and colleagues (Figure 14) (157).

In Zone 1, P_{ALV} exceeds both P_{C-I} and P_{C-O}, P_{C-TM} is uniformly negative, the capillaries are collapsed, and there is no blood flow. In Zone 2, P_{C-I} exceeds P_{ALV}, but as P_{C-IM} falls with blood flow, P_{C-TM} becomes negative. Permutt and co-workers (109) showed that under Zone-2 conditions, the capillaries develop *flow limitation*. That is, they flutter between opening and closing, and blood flow is determined by the gradient between P_{C-I} and P_{ALV}, not P_{C-I} and P_{C-O}. This is often referred to as a "vascular waterfall" because flow over the precipice of a waterfall is determined by the slope of the riverbed ($P_{C-I} - P_{ALV}$) not by the height of the waterfall ($P_{ALV} - P_{C-O}$) (109). Thus, P_{ALV} becomes the back pressure for blood flow in both Zone-1 and Zone-2 capillaries. In Zone 3, P_{C-I} and P_{C-O} exceed P_{ALV}, P_{C-TM} is uniformly positive, and blood flow is driven by the difference between P_{C-I} and P_{C-O}.

The Effects of Mechanical Ventilation on the Cardiovascular System

Pleural, alveolar, and intra-abdominal pressure define the "compartments" of the cardiovascular system. Changes in these extramural pressures during spontaneous and mechanical ventilation alter venous return and RV and LV preload and afterload. The resulting hemodynamic changes define the respiratory-cardiovascular interactions. With positive-pressure inflation and PEEP,

- The rise in P_{PL} reduces venous return and RV preload.
- The rise in P_{L-TM} and P_{ALV} increases RV afterload.
- The rise in P_{PL} decreases LV afterload.
- The fall in RV preload and rise in RV afterload reduce RV stroke volume, which decreases LV preload and stroke volume after several cardiac cycles.

The hemodynamic effects of a passive mechanical breath are shown schematically in Figure 15.

Positive end-expiratory pressure elevates P_{ALV}, P_{PL}, P_{L-TM}, and P_{AB} throughout the entire respiratory cycle rather than only during inspiration (Figure 4B). Thus, its hemodynamic effects are usually greater than those produced by intermittent, positive-pressure breaths alone and increase in proportion to $PEEP_T$.

Right ventricular preload

It has long been recognized that positive-pressure ventilation and PEEP decrease systemic venous return and RV preload in proportion to the rise in P_{PL} (38, 39, 111, 112). Based on Guyton's model, this has traditionally been attributed to the resulting increase in P_{RA-IM}, which reduces the pressure gradient driving venous return (Eq. 15). Unfortunately, it is almost certainly not that simple. Experiments in both animal models (39, 40, 94) and humans (64, 118, 142) have shown that P_{MS} and P_{RA-IM} increase by about the same amount during positive-pressure inflation (118), with increasing levels of PEEP (39, 40, 94, 118), and when positive airway pressure is applied during apnea (64, 142). Thus, venous return is decreased, apparently without changing its driving pressure.

Although experimental evidence is inconclusive, it is likely that one or more of the following factors are responsible for the rise in P_{MS}: (i) blood is transferred from the alveolar vessels to the systemic circulation by the increase in P_{ALV} and fall in P_{C-TM} (39, 64, 118); (ii) increasing P_{AB} raises the pressure within the splanchnic venous reservoir (118, 142); and (iii) autonomic reflexes respond to a fall in blood pressure by increasing venous tone and reducing venous capacitance (39, 94, 118). Since reflex venoconstriction does not occur immediately (94), it is unlikely to contribute to the rise in P_{MS} during individual mechanical breaths.

The mechanism(s) by which positive airway pressure reduces venous return also remains unclear. Based on Eq. (15), if the driving pressure is unchanged, decreased venous return must be caused by increased resistance, and this has been reported by several investigators (40, 94). Another possible explanation is that by increasing P_{PL} and P_{AB}, positive pressure inflation and PEEP favor the formation of vascular waterfalls in the SVC and IVC (37, 39, 40, 134, 135, 145).

Like the pulmonary capillaries, when P_{SVC-IM} and P_{IVC-IM} exceed P_{PL} and P_{AB}, respectively (as in Figure 13), venous transmural pressures are uniformly positive, and Zone 3 conditions are present. Thus, P_{RA-IM} is the back pressure for venous return, and increased flow from the splanchnic reservoir may partially or completely compensate for reduced flow from the extra-thoracic and extra-abdominal veins (142). However, when extramural pressure exceeds P_{SVC-IM} or P_{IVC-IM}, Zone-2 conditions are present, flow limitation occurs, and P_{PL}, P_{AB}, or both become the back pressure for venous return. Thus, the true driving pressure for venous return falls. Studies have shown that a vascular waterfall can form within the SVC in some mechanically

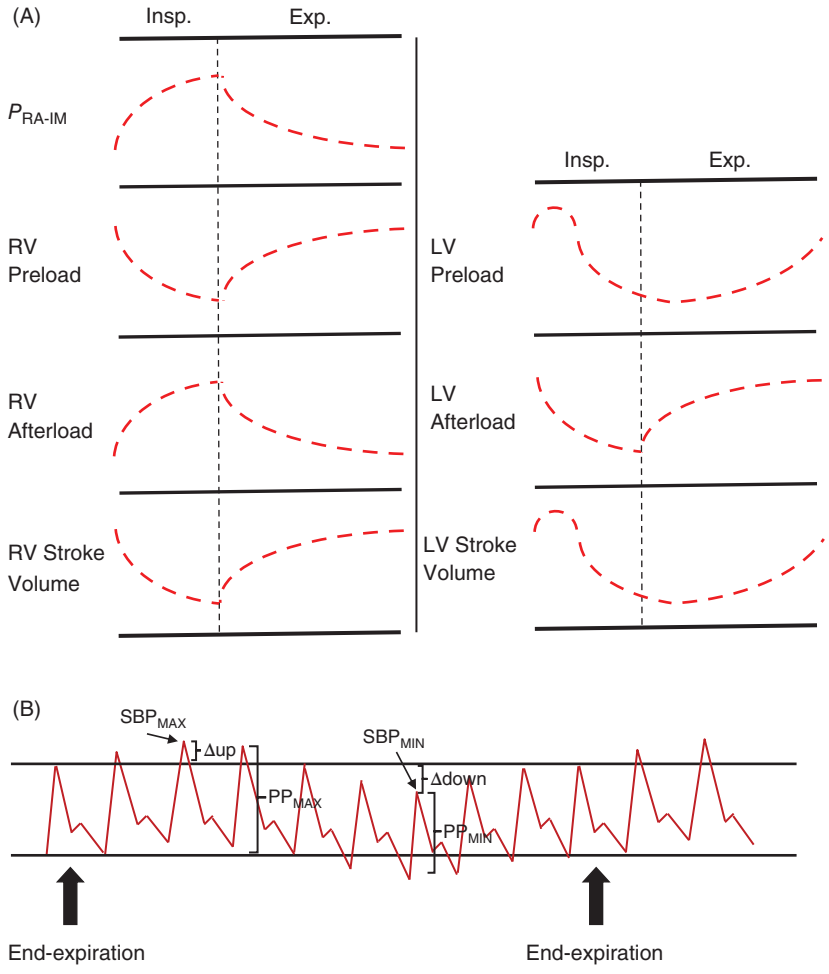

Figure 15 (A) Schematic representation of the changes in right atrial intramural pressure (P_{RA-IM}) and right and left ventricular (RV, LV) preload, afterload, and stroke volume during a passive, positive-pressure breath. Insp., inspiration; Exp., expiration. (B) Schematic representation of changes in systemic blood pressure during a passive, positive-pressure breath. The maximal (SBP_{MAX}) and minimal (SBP_{MIN}) systolic blood pressure, the maximal increase (Δup) and decrease (Δdown) in systolic blood pressure from end expiration, and the maximal (PP_{MAX}) and minimal (PP_{MIN}) pulse pressure are shown (see later section: Blood pressure). From Kreit J. Mechanical Ventilation. Oxford University Press, 2018. Reproduced with permission of the licensor through PLSclear.

ventilated patients (145, 147), and an IVC waterfall has been demonstrated in mechanically ventilated dogs (134, 135) and in spontaneously breathing patients during an acute asthma exacerbation (60).

Right ventricular afterload

Experimental data obtained using isolated animal lungs and intact animal preparations have shown that alveolar vessels are compressed (56, 107), extra-alveolar vessels dilate (8, 44, 52, 56, 107, 131), and total PVR increases (18, 28, 52, 56, 70, 110, 120, 140, 158) with $P_{L\text{-}TM}$ during both negative- and positive-pressure inflation. In these studies, negative-pressure inflation was performed by lowering the pressure surrounding the isolated lung or the thorax below P_{ATM} to simulate a spontaneous breath. Although conclusions based on experimental data have been far from uniform (52, 110, 120), consensus has emerged that (i) PVR is lowest near the equilibrium volume of the respiratory system and increases at higher and lower lung transmural pressures and volumes; and (ii) the relationship between $P_{L\text{-}TM}$, the resistance of the alveolar and the extra-alveolar vessels, and total PVR is the same during spontaneous and mechanical breaths (41, 75, 115). These relationships are illustrated by figures that have become ubiquitous in physiology and clinical texts (Figure 16), even though the original data came from a single study performed on ten mechanically ventilated dogs (129).

From a theoretical standpoint, the relationship between $P_{L\text{-}TM}$ and the caliber of the alveolar and extra-alveolar vessels should, in fact, be the same. During spontaneous inspiration, P_{PL} falls more than P_{ALV} as $P_{L\text{-}TM}$ increases (Figure 3). Since the LA is exposed to P_{PL}, $P_{LA\text{-}IM}$ and

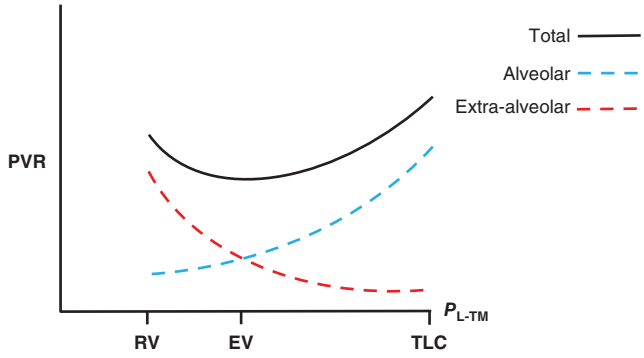

Figure 16 The change in alveolar, extra-alveolar, and total pulmonary vascular resistance (PVR) as lung transmural pressure ($P_{L\text{-}TM}$) increases from residual volume (RV) to total lung capacity (TLC). Total PVR is lowest near the equilibrium volume of the respiratory system (EV), which is normally functional residual capacity. Based on, with permission, Fishman AP, 2011 (41); Lumb AB, 2010 (75); Purmutt S and Wise RA, 2011 (115).

"upstream" $P_{C\text{-}IM}$ also fall more than P_{ALV}. This reduces $P_{C\text{-}TM}$, which shifts alveolar capillaries from Zones 2 and 3 to Zones 1 and 2 (56, 107). The extra-alveolar vessels are attached to innumerable alveolar septa as they course through the lung parenchyma. Although these vessels are exposed to P_{PL}, like the bronchioles, their caliber is determined by the pull or radial traction exerted by the adjacent lung (8, 56, 107). Thus, the resistance of the intra-parenchymal pulmonary arteries and veins falls as lung volume and $P_{L\text{-}TM}$ increase (56, 107, 158). With mechanical breaths and PEEP, $P_{L\text{-}TM}$ increases because P_{ALV} rises more than P_{PL} (Figure 4), but the effect on the alveolar and extra-alveolar vessels is the same: P_{ALV} increases more than $P_{LA\text{-}IM}$ and $P_{C\text{-}IM}$, $P_{C\text{-}TM}$ falls, and the number of Zone-3 capillaries decreases, while the extra-alveolar vessels dilate with increasing lung volume.

Although the relationship between PVR and $P_{L\text{-}TM}$ is probably the same, two factors may significantly increase RV afterload during mechanical ventilation. First, P_{ALV} increases with positive-pressure inflation and PEEP. Because P_{ALV} is the back pressure within Zone-1 and Zone-2 capillaries, the RV must contract against a higher pressure that increases throughout inspiration and in proportion to $PEEP_T$. Second, by raising end-expiratory and end-inspiratory lung volume, PEEP causes a rightward shift on the PVR-$P_{L\text{-}TM}$ curve and an exponential rise in PVR. During positive-pressure inflation, the increase in RV afterload combined with the fall in RV preload reduces RV stroke volume (59, 149).

Left ventricular preload and afterload

Left ventricular preload initially rises during mechanical inflation because the decrease in $P_{C\text{-}TM}$ and the collapse of alveolar vessels pushes blood into the LA (16, 56, 107); preload subsequently falls with the drop in RV stroke volume. Left ventricular afterload falls during positive-pressure inflation and in proportion to $PEEP_T$ because the rise in P_{PL} increases the pressure within the LV during the isovolumic phase of systole (Figure 17). Therefore, the LV must generate less intramural pressure to eject the stroke volume, and systolic transmural pressure and wall stress fall (17, 38, 113, 114). The combination of increased LV preload and decreased LV afterload augments LV stroke volume at the onset of inspiration. Stroke volume then falls as less blood is delivered by the RV.

Blood pressure

Changes in systemic blood pressure (BP) (Figure 15B) mirror those of LV stroke volume (58, 105, 106). Increased LV preload and decreased LV afterload are responsible for the normal rise in systolic BP and pulse pressure at the onset of mechanical inflation. Left ventricular stroke volume, systolic BP, and pulse pressure then fall with the decrease in RV output and reach their nadir after several cardiac cycles, usually in early expiration. This normal physiological response is minimal or absent when one or both ventricles are functioning on the plateau of their respective Starling curves (4).

Factors influencing the hemodynamic effects of mechanical ventilation

Tidal volume, PEEP, and compliance

Recall from Figures 1 and 2 that P_{ALV} ($P_{RS\text{-}TM}$) equals the sum of P_{PL} ($P_{CW\text{-}TM}$) and $P_{L\text{-}TM}$. During positive-pressure inflation, the increase in alveolar pressure (ΔP_{ALV}) varies directly with tidal volume (V_T) and inversely with respiratory system compliance (Eq. 3), but its two components, ΔP_{PL} and $\Delta P_{L\text{-}TM}$, vary inversely with chest wall and lung compliance, respectively. This is illustrated by the static V-P_{TM} curves shown in Figure 18. When chest wall and lung compliance are normal (Figure 18A), ΔP_{PL} and $\Delta P_{L\text{-}TM}$ during a passive, positive-pressure breath are similar. When V_T is constant and chest wall compliance falls (Figure 18B), ΔP_{PL} increases without changing $\Delta P_{L\text{-}TM}$. When lung compliance decreases (Figure 18C) at constant V_T, $\Delta P_{L\text{-}TM}$ increases without changing ΔP_{PL}. Thus, a mechanical breath has a greater effect on ventricular preload and LV afterload when chest wall compliance is low and a greater effect on right ventricular afterload when lung compliance is low.

Positive end-expiratory pressure produces an identical increase in P_{ALV}, (i.e., $PEEP = \Delta P_{ALV}$) but the resulting rise in P_{PL} and $P_{L\text{-}TM}$ are, once again, determined by lung and chest wall compliance (Figure 19) (20, 61, 96). When chest wall and lung compliance are normal (Figure 19A), ΔP_{PL} and $\Delta P_{L\text{-}TM}$ are approximately equal. When chest wall compliance is reduced (Figure 19B) or lung compliance is increased (Figure 19C), ΔP_{PL} becomes a larger portion and $\Delta P_{L\text{-}TM}$ becomes a smaller portion of ΔP_{ALV}. Thus, PEEP has a greater effect on ventricular preload and LV afterload than on RV afterload. When lung compliance is low (Figure 19D) or

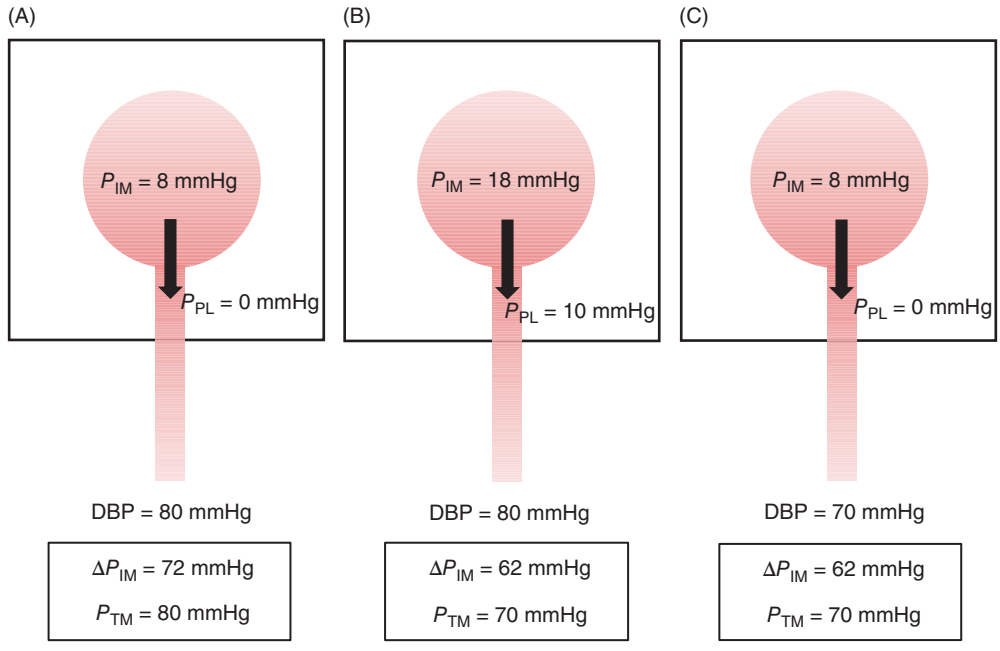

Figure 17 Illustration showing the left ventricle (circle) and the aorta (narrow rectangle). The ventricle and proximal aorta are within the thorax (black square) and exposed to pleural pressure (P_{PL}). The intramural left ventricular end-diastolic pressure (P_{IM}) and the diastolic blood pressure (DBP) are shown. (A) In this example, when P_{PL} is 0 mmHg, the LV must increase its intramural pressure (ΔP_{IM}) by 72 mmHg during isovolumic contraction to open the aortic valve, and, at the onset of the ejection phase, ventricular transmural pressure (P_{TM}) is 80 mmHg. (B) When P_{PL} increases to 10 mmHg, P_{IM} rises by the same amount during isovolumic contraction. Since DBP does not change, the ventricle must generate only 62 mmHg, P_{TM} decreases to 70 mmHg, and LV afterload falls. (C) Reducing DBP by 10 mmHg has the same effect on ΔP_{IM}, P_{TM}, and LV afterload as increasing P_{PL} by 10 mmHg.

chest wall compliance is high (e.g., a "flail" chest caused by multiple rib fractures), $\Delta P_{L\text{-}TM}$ becomes a larger portion and ΔP_{PL} becomes a smaller portion of ΔP_{ALV}, and PEEP has a greater effect on RV afterload than on ventricular preload and LV afterload.

The relationship between PEEP, ΔP_{PL}, $\Delta P_{L\text{-}TM}$, and respiratory system mechanics can also be derived mathematically (61). Elastance (E), the reciprocal of compliance, is used because the equations require the sum of lung and chest wall elastance to equal respiratory system elastance; this is not true of lung and chest wall compliance.

$$E = \Delta P_{TM}/\Delta V \tag{17}$$

Rearranging and substituting into Eq. (17) shows that the change in $P_{L\text{-}TM}$, $P_{CW\text{-}TM}$, and $P_{RS\text{-}TM}$ equals the product of ΔV and the elastance of the lungs (E_L), chest wall (E_{CW}), and respiratory system (E_{RS}), respectively.

$$\Delta P_{L\text{-}TM} = E_L \times \Delta V$$
$$\Delta P_{CW\text{-}TM} = \Delta P_{PL} = E_{CW} \times \Delta V$$
$$\Delta P_{RS\text{-}TM} = \Delta P_{ALV} = E_{RS} \times \Delta V$$

Because ΔV is the same in these three equations,

$$\Delta V = \Delta P_{PL}/E_{CW} = \Delta P_{L\text{-}TM}/E_L = \Delta P_{ALV}/E_{RS}$$

Thus,

$$\Delta P_{PL}/E_{CW} = \Delta P_{ALV}/E_{RS}$$

and

$$\Delta P_{L\text{-}TM}/E_L = \Delta P_{ALV}/E_{RS}$$

which can be rearranged to give

$$\Delta P_{PL} = \Delta P_{ALV} \times E_{CW}/E_{RS} = \Delta P_{ALV} \times E_{CW}/(E_{CW} + E_L)$$

and

$$\Delta P_{L\text{-}TM} = \Delta P_{ALV} \times E_L/E_{RS} = \Delta P_{ALV} \times E_L/(E_{CW} + E_L)$$

Since PEEP equals ΔP_{ALV}, these equations can be rewritten as

$$\Delta P_{PL} = \text{PEEP} \times E_{CW}/(E_{CW} + E_L) \tag{18}$$

and

$$\Delta P_{L\text{-}TM} = \text{PEEP} \times E_L/(E_{CW} + E_L) \tag{19}$$

Thus, ΔP_{PL} rises disproportionately with PEEP as chest wall elastance increases (compliance decreases) or lung elastance decreases (compliance increases), and $\Delta P_{L\text{-}TM}$ rises disproportionately as lung elastance increases (compliance decreases) or chest wall elastance decreases (compliance increases).

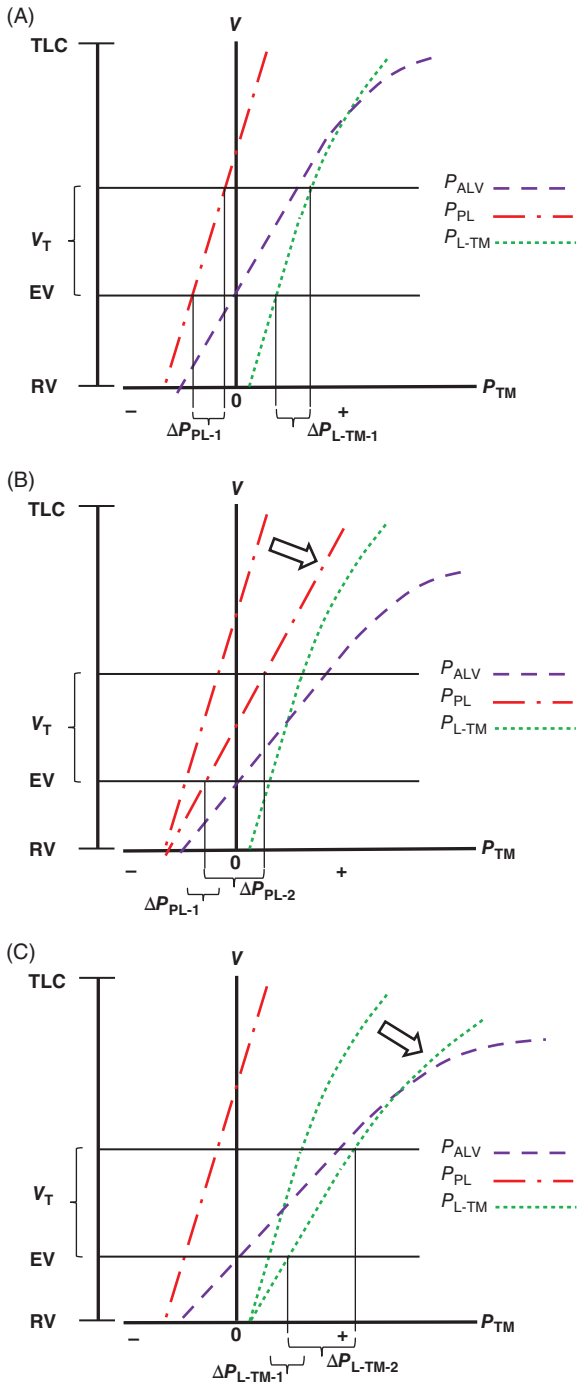

Figure 18 (A) Normal, static, expiratory volume-transmural pressure curves of the lungs, chest wall, and respiratory system showing the increase in pleural pressure ($\Delta P_{PL\text{-}1}$) and lung transmural pressure ($\Delta P_{L\text{-}TM\text{-}1}$) during tidal inflation. When tidal volume (V_T) is constant, a decrease (arrows) in chest wall (B) or lung (C) compliance (i.e., a decrease in slope) reduces the equilibrium volume (EV) of the respiratory system and causes a larger tidal increase in pleural pressure ($\Delta P_{PL\text{-}2} > \Delta P_{PL\text{-}1}$) and lung transmural pressure ($\Delta P_{L\text{-}TM\text{-}2} > \Delta P_{L\text{-}TM\text{-}1}$), respectively. P_{TM}, transmural pressure; P_{ALV}, alveolar pressure; $P_{L\text{-}TM}$, lung transmural pressure; P_{PL}, pleural pressure; V, volume; V_T, tidal volume; TLC, total lung capacity; RV, residual volume; +, positive transmural pressure; –, negative transmural pressure. From Kreit J. Mechanical Ventilation. Oxford University Press, 2018. Reproduced with permission of the licensor through PLSclear.

Intravascular volume

The ventricles normally function on the steep portion of the Starling curve. Thus, the positive-pressure-induced reduction in venous return and ventricular preload is more prominent in hypovolemic or euvolemic patients and reduced or eliminated by hypervolemia. Hypovolemia further magnifies the effect of mechanical ventilation on RV function because (i) vascular waterfalls are more likely to occur in the intrathoracic and intra-abdominal veins (37, 39, 40, 134, 135, 145); and (ii) reduced $P_{C\text{-}IM}$ and $P_{C\text{-}TM}$ increase the number of Zone-1 and Zone-2 capillaries, thereby raising the back pressure for flow through the pulmonary circuit and increasing RV afterload (120, 158).

Right and left ventricular function

With its thin free wall and small muscle mass, the normal RV is incapable of acutely generating high intraventricular pressures. Thus, patients with preexisting RV dysfunction are much more susceptible to positive-pressure-induced increases in RV afterload. As shown in Figure 11, when contractility is reduced, the Starling curve and the ventricle's "position" on it shift downward and to the right; this increases preload, and the RV approaches or reaches the curve's plateau. Thus, when an increase in afterload further reduces stroke volume and pushes the RV to the right along the plateau of its function curve, the ventricle cannot restore stroke volume by additional increases in preload. Conversely, patients with LV systolic dysfunction are likely to benefit from the fall in LV preload and afterload produced by a rise in P_{PL}.

Intra-abdominal pressure

Abnormally high P_{AB} pushes the diaphragm upward, thereby decreasing intrathoracic volume and increasing P_{PL}; it also predisposes to Zone-2 conditions in the IVC (134, 135). Thus, the decrease in ventricular preload and stroke volume produced by mechanical ventilation and PEEP may be exaggerated in the presence of intra-abdominal hypertension.

Important Respiratory-cardiovascular Interactions in Mechanically Ventilated Patients

Acute respiratory distress syndrome

Since it was first recognized as an effective therapy in 1967 (5), PEEP has played an important role in the management of patients with acute hypoxemic respiratory failure. By increasing P_{ALV} and the equilibrium volume of the respiratory system, PEEP opens or "recruits" atelectatic alveoli throughout the respiratory cycle, thereby reducing the shunt fraction and improving arterial hemoglobin saturation and O_2 content. An optimal level of PEEP may also reduce

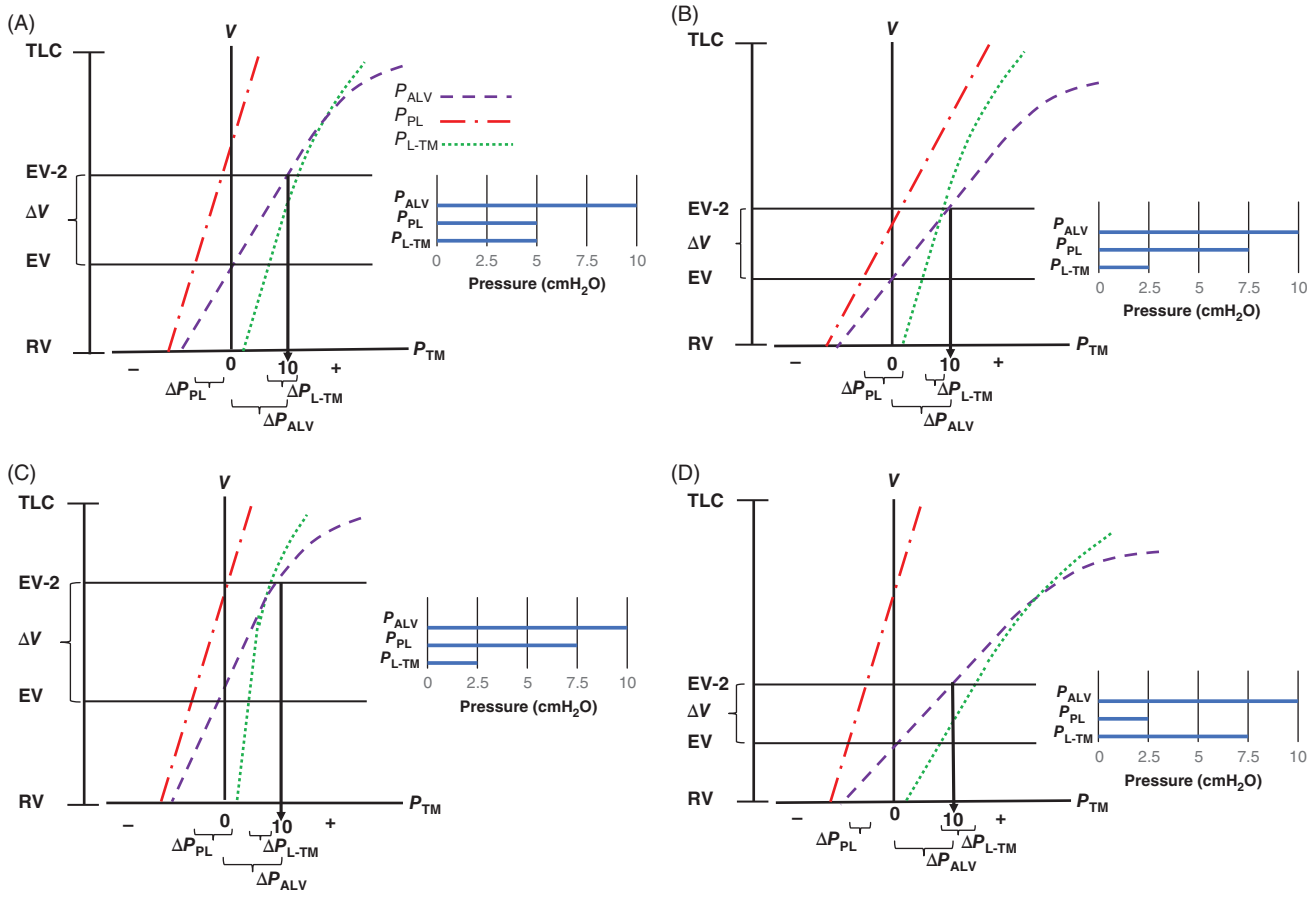

Figure 19 Static, expiratory volume-transmural pressure curves of the lungs, chest wall, and respiratory system showing normal lung and chest wall compliance (A), decreased chest wall compliance (B), increased lung compliance (C), and decreased lung compliance (D). In each figure, the new equilibrium volume (EV-2) produced by PEEP of 10 cmH_2O (arrow) and the resulting volume increase (ΔV) above the original equilibrium volume (EV) are shown. Also shown is the partitioning of the increase in alveolar pressure ($\Delta P_{ALV} = 10\,cmH_2O$) between the increase in pleural (ΔP_{PL}) and lung transmural ($\Delta P_{L\text{-}TM}$) pressure. Note that PEEP = ΔP_{ALV} and $\Delta P_{ALV} = \Delta P_{PL} + \Delta P_{L\text{-}TM}$. *V*, volume; P_{TM}, transmural pressure; TLC, total lung capacity; RV, residual volume; +, positive transmural pressure; –, negative transmural pressure. Based on, with permission, Chapin JC, et al., 1979 (20); Jardin F, et al., 1985 (61); O'Quinn RJ, et al., 1985 (96).

ventilator-induced lung injury by preventing alveolar recruitment and de-recruitment during each ventilatory cycle (130). Unfortunately, by elevating P_{ALV}, PEEP also increases both P_{PL}, which reduces ventricular preload, and $P_{L\text{-}TM}$, which increases RV afterload. Based on the principles discussed in the preceding section, the type and severity of adverse hemodynamic effects are determined by $PEEP_T$, lung and chest wall compliance, intravascular volume, intra-abdominal pressure, and baseline RV and LV function.

Lung compliance is decreased in patients with the acute respiratory distress syndrome (ARDS) (103, 117); thus, FRC is reduced, and PEEP proportionally increases $P_{L\text{-}TM}$ more than P_{PL} (Figure 19D) (59, 61). This probably explains the clinical observation that even high levels of PEEP usually have relatively little effect on cardiac output and BP in the absence of significant hypovolemia (59, 149). Studies separating ARDS patients based on underlying cause (43, 117) have shown that chest wall compliance is usually normal in those with primary lung disease (e.g., pneumonia) but reduced in those with extra-pulmonary causes (e.g., pancreatitis, intra-abdominal infection, abdominal trauma) that predispose to abdominal distention and intra-abdominal hypertension. Thus, PEEP would cause a greater rise in P_{PL} (Figure 19B), and patients with extra-pulmonary ARDS would be expected to have a higher risk of PEEP-induced hypotension (43).

Prone positioning reduces chest wall compliance and increases P_{AB} by limiting movement of the anterior chest and abdominal walls and may increase lung compliance by augmenting alveolar recruitment (53, 90, 104). When used during surgical procedures, prone positioning decreases cardiac output, primarily through a reduction in venous return (6, 141). However, in physiological studies (13, 53, 104) and randomized, clinical trials (46) of ARDS patients, prone ventilation has rarely had adverse hemodynamic effects and may even increase ventricular preload (66), cardiac output (53, 66),

and BP (66), especially in volume-responsive patients. Possible explanations include patient selection, routine volume resuscitation prior to prone positioning, reduced PEEP requirement (146) while prone, and the more dependent position of the RA, SVC, and IVC when supine, semi-recumbent patients are moved to the prone position (2, 77). Despite its apparent safety, vigilance is advised when implementing prone ventilation in patients with hypovolemia, reduced chest wall compliance (e.g., morbid obesity, extra-pulmonary ARDS), or intra-abdominal hypertension.

Although lung injury and acute respiratory failure dominate the clinical picture, ARDS also has significant, adverse effects on the pulmonary circulation and the heart (163, 164). Vascular damage and thrombosis, and vasoconstriction induced by alveolar hypoxia and hypercapnia and the local release of vasoactive mediators, increase RV afterload by elevating PVR (163, 164). When $P_{L\text{-}TM}$ is disproportionately increased, mechanical ventilation and PEEP further elevate RV outflow impedance and may precipitate acute RV dysfunction (59, 149, 151).

During the latter part of the twentieth century, studies confirmed that pulmonary hypertension and RV dysfunction were common in patients with ARDS (62, 152, 163). In the era of low-tidal-volume ventilation, the prevalence has fallen, but *acute cor pulmonale* (ACP), which, in research studies, is usually defined by transesophageal echocardiography as RV/LV chamber area greater than 0.6 accompanied by leftward septal shift, still occurs in approximately 25% of patients (15, 74, 88). Acute cor pulmonale has been identified as an independent risk factor for mortality in some studies (15, 63, 88, 97) but not in others (74, 151). In the largest study to date, mortality increased only when RV/LV chamber area exceeded 1.0; this was present in 11% of patients (88).

In agreement with previously discussed physiological principles, identified risk factors for ACP include (i) high V_T; (ii) high $PEEP_T$; (iii) low lung compliance; (iv) elevated end-inspiratory P_{ALV} (plateau pressure), which incorporates V_T, $PEEP_T$, and lung compliance; and (v) increased driving pressure (plateau pressure minus $PEEP_T$), which incorporates V_T and lung compliance (15, 88, 89, 125). The prevalence of ACP also increases with arterial hypercapnia (62, 74, 88, 89), which causes pulmonary vasoconstriction, and ARDS severity (88), presumably because of worsening pulmonary vascular injury, increasing alveolar hypoxia- and hypercapnia-induced vasoconstriction, decreasing lung compliance, and higher PEEP requirements. Elevated intravascular volume may also be a risk factor for ACP by predisposing to RV volume and pressure overload.

To reduce the risk of ACP, a management strategy called "RV-protective ventilation" has been proposed (100, 150). This approach seeks to reduce RV afterload by avoiding hypercapnia and by using low V_T and driving pressure and the lowest PEEP needed to optimize alveolar recruitment. Recommended goals are plateau pressure less than 27 cmH_2O (63), driving pressure less than 18 cmH_2O (146), and $PaCO_2$ less than 48 mmHg (88).

Prone positioning is also an important component of RV protective ventilation because it reduces RV afterload, decreases RV size, and improves RV function in patients with severe ARDS (146). These beneficial effects have been attributed to a decrease in $\Delta P_{L\text{-}TM}$ produced by (i) the fall in chest wall compliance; (ii) the increase in lung compliance from enhanced alveolar recruitment; and (iii) a decrease in the required level of PEEP (100, 150). The impact of RV protective ventilation on patient outcomes has not been evaluated.

Obstructive lung disease

Patients with chronic obstructive pulmonary disease, acute asthma, bronchiectasis, and bronchiolitis may develop dynamic hyperinflation and intrinsic PEEP during mechanical ventilation (82). Clinical experience indicates that these patients, at similar levels of $PEEP_T$, are much more likely to develop preload-mediated hypotension than patients with ARDS. This is explained by the difference in lung compliance, not by a difference between intrinsic and extrinsic PEEP. When lung compliance is low (Figure 19D), a set level of PEEP has a relatively small effect on P_{PL} and ventricular preload. When lung compliance is normal (Figure 19A) or high (Figure 19C), as in emphysema, the same level of (intrinsic) PEEP causes a larger increase in P_{PL} and is more likely to reduce ventricular preload, stroke volume, and BP (20).

Pulmonary hypertension and right ventricular failure

Although the normal RV is incapable of acutely generating high intraventricular pressures, it has a remarkable ability to adapt to gradually increasing pulmonary arterial pressure through concentric hypertrophy, which, according to the law of LaPlace, reduces wall stress and afterload (121, 139, 153, 154). Although hypertrophy can preserve ventricular function by reducing afterload, it predisposes to RV ischemia as increased RV mass raises myocardial O_2 requirements, and high intraventricular pressures reduce coronary blood flow.

In patients with chronic pulmonary hypertension or acute RV dysfunction (e.g., RV infarction or pulmonary embolism), overt RV failure can be precipitated by a sudden decrease in RV contractility, an acute increase in afterload, or both. In response, end-diastolic volume rises and the RV dilates, which increases RV wall stress and afterload, worsens tricuspid regurgitation, and impairs LV filling through a leftward shift of the interventricular septum. This triggers a vicious cycle with a progressive fall in LV stroke volume, cardiac output, and BP (121, 139, 153, 154).

One of the most common causes of acute RV failure in at-risk patients is intubation and mechanical ventilation. This feared complication is usually attributed to the sudden

increase in RV afterload produced by positive-pressure ventilation, although sedatives, anesthetics, and narcotics administered before and after intubation probably contribute by directly depressing myocardial function, inducing RV ischemia through a reduction in systemic BP, or both (22, 27, 55, 124, 143). Based on previously discussed principles, baseline RV dysfunction and low lung compliance (e.g., interstitial lung disease) significantly increase the risk of acute RV failure.

Little data is available to guide therapy, and expert opinion focuses primarily on prevention (22, 27, 55, 69, 124, 143). The most effective measure, of course, is to avoid mechanical ventilation, and the importance of early, extracorporeal support in appropriate patients has been emphasized (55). If mechanical ventilation is required, several measures may reduce the risk of acute RV failure (22, 27, 55, 124). First, noninvasive ventilation, which does not require patient sedation, should be used, if possible. Second, intubation should be performed using etomidate, a rapidly acting anesthetic with minimal cardiovascular effects, and sedation during mechanical ventilation should be minimized to reduce the risk of drug-induced hypotension. Third, a continuous norepinephrine infusion should be used, if necessary, to produce mild hypertension prior to intubation. In the hypertensive patient, norepinephrine must be immediately available during and after intubation to rapidly correct systemic hypotension and prevent RV ischemia. Fourth, the increase in RV afterload should be limited by maintaining low V_T and by minimizing or (preferably) avoiding PEEP. Finally, the ventilator rate should be adjusted to minimize hypercapnia and acidemia, which increase PVR.

Recommended therapies for established, ventilator-induced RV failure include inhaled nitric oxide or epoprostenol to reduce RV afterload, an intravenous inotrope, such as dobutamine (68) to increase RV contractility, and norepinephrine to increase RV perfusion by maintaining a gradient between systemic arterial pressure and RV systolic pressure (22, 27, 55, 69, 124, 143). Serial assessments of RV function using echocardiography or right heart catheterization may help to guide therapy (69).

Cardiogenic pulmonary edema

In patients with decompensated systolic heart failure and pulmonary edema, the LV functions far to the right on the plateau of a depressed Starling curve. Thus, LV end-diastolic pressure and pulmonary capillary pressure are markedly elevated, and stroke volume and cardiac output are low. Diuretics and nitrates treat pulmonary edema without further reducing stroke volume by moving the "position" of the LV to the left along the plateau of the Starling curve. Arterial vasodilators assist the failing heart by decreasing LV afterload, which increases stroke volume and further reduces LV and pulmonary capillary pressure.

It has long been recognized that invasive and noninvasive mechanical ventilation rapidly improve dyspnea and tachypnea in patients with cardiogenic pulmonary edema (45, 84, 95). Although this could logically be attributed to mechanical ventilatory support, similar benefits are achieved using continuous positive airway pressure (CPAP), which provides no ventilatory assistance (33, 99). The explanation is straightforward. By increasing P_{PL}, CPAP and mechanical ventilation, like diuretics, nitrates, and arterial vasodilators, directly assist the failing LV by reducing RV and LV preload and LV afterload in proportion to the applied airway pressure. Meta-analyses of mostly small, randomized trials have concluded that CPAP and noninvasive mechanical ventilation (NIV) also reduce both the need for intubation and hospital mortality in patients with cardiogenic pulmonary edema (9, 156).

When positive-pressure therapy is stopped, the negative P_{PL} during spontaneous breaths abruptly increases venous return and LV preload and afterload. When the heart is unable to compensate, the rise in LV end-diastolic and pulmonary capillary pressure initiates a vicious cycle in which respiratory distress further decreases inspiratory P_{PL} and activates the sympathetic nervous system, which increases heart rate, blood pressure, and myocardial O_2 demand (3, 67, 73). Thus, it is not surprising that patients with LV systolic dysfunction may develop pulmonary edema and acute respiratory failure following extubation or when CPAP or NIV are stopped. Furthermore, occult LV dysfunction can cause persistent ventilator dependence even when respiratory parameters, such as spontaneous V_T, respiratory rate, and vital capacity indicate the ability to maintain spontaneous ventilation (67, 73). This has led to the practice of gradually reducing mask-delivered airway pressure and performing truly spontaneous (i.e., T-piece) breathing trials in intubated patients. Patients who fail initial attempts can usually be successfully liberated from positive-pressure therapy after aggressive diuresis (3, 73). In many cases, diuresis to the point of prerenal azotemia is needed.

Assessing volume responsiveness

Intravenous (IV) fluid is an essential therapy for many patients with hypotension and shock. In the presence of hypovolemia, volume expansion increases systemic venous return, RV and LV preload and stroke volume, cardiac output, BP, and tissue O_2 delivery. Excessive IV fluids, however, are unlikely to further increase cardiac output and may cause tissue and pulmonary edema, worsen oxygenation, and increase the duration of mechanical ventilation (159). Thus, it is important to determine if hypotensive patients are *volume responsive*—that is, whether they are likely to have a clinically significant increase in stroke volume following volume infusion. Physical examination and static measurements such as central venous pressure, pulmonary artery wedge pressure, ventricular end-diastolic volume, and end-expiratory IVC diameter are unreliable indicators of volume responsiveness (80, 148). However, several dynamic measurements that assess the response to a change in ventricular preload have

been shown to accurately predict the response to volume expansion (127).

Although many dynamic measurements have been studied, all have the same physiological basis. The Starling curve dictates that a change in preload alters stroke volume only when the ventricle is functioning on the steep portion of the Starling curve, not when it has reached its plateau. Thus, all measurements quantify the change in stroke volume, cardiac output, or a surrogate following a transient change in ventricular end-diastolic pressure and volume; they differ in the measurements performed and the way in which ventricular preload is altered. Several, commonly used, predictive tests rely on respiratory-cardiovascular interactions, and these will be discussed here.

Systolic pressure variation

The systolic pressure variation (SPV) is the difference between the maximal and minimal systolic arterial pressure during a passive mechanical breath (Figure 15B). It is the sum of the initial rise in systolic pressure from its end-expiratory value (Δup) and the subsequent fall below end-expiratory systolic pressure (Δdown). Systolic pressure variation and Δdown, but not Δup, are highly correlated with the volume of blood removed during stepwise hemorrhage in dogs (106) and with volume responsiveness in critically ill patients (81). Thus, Δdown, which reflects the positive-pressure-induced drop in RV and LV preload and stroke volume, accounts for the predictive value of the SPV.

Pulse pressure variation

Arterial pulse pressure (PP), the difference between systolic and diastolic pressure, is directly proportional to LV stroke volume and inversely related to aortic compliance (138). Thus, during passive mechanical ventilation, pulse pressure is highest during inspiration and lowest during expiration (Figure 15B). The pulse pressure variation (PPV), expressed as a percentage, is calculated by dividing the difference between the maximum (PP_{MAX}) and minimum (PP_{MIN}) pulse pressure by their average.

$$PPV(\%) = [(PP_{MAX} - PP_{MIN})/[(PP_{MAX} + PP_{MIN})/2]] \times 100 \quad (20)$$

Studies have shown a highly significant, positive correlation between PPV and the increase in stroke volume or cardiac output following an IV fluid bolus (138). Most have arbitrarily defined volume responsiveness as an increase in stroke volume or cardiac output of at least 15% and have identified a threshold PPV that best separates volume-responsive from nonresponsive patients. A meta-analysis published in 2014 included 22 trials with a total of 807 critically ill patients who were passively ventilated with a V_T of at least 8 mL/kg (162). Based on the pooled data, the threshold PPV was 12%, and pooled sensitivity and specificity were 0.88 and 0.89, respectively.

Stroke volume variation

This calculation is identical to PPV except that stroke volume (SV) is repeatedly measured during passive mechanical ventilation, and SV_{MAX} and SV_{MIN} are substituted for PP_{MAX} and PP_{MIN} in Eq. (20). Like SPV and PPV, clinical studies have shown an excellent correlation between stroke volume variation (SVV) and the increase in stroke volume or cardiac output following volume infusion (81). A meta-analysis published in 2009 found a mean SVV threshold of 12% and a pooled sensitivity and specificity of 0.82 and 0.86, respectively for a volume-induced increase in stroke volume or cardiac output of at least 15% (81). A major source of heterogeneity among clinical studies is the method used to calculate stroke volume; techniques have included thermodilution, pulse contour analysis, esophageal Doppler, and bioimpedance (123).

Inferior vena cava diameter

The ventilation-induced increase in the diameter of the intra-hepatic IVC during passive mechanical breaths also predicts volume responsiveness (7, 128). Ultrasound is used to obtain a long-axis view of the IVC from the subcostal window, and M-mode is used to measure its maximum (IVC_{MAX}) and minimum (IVC_{MIN}) diameter during the respiratory cycle. A meta-analysis published in 2018 evaluated 12 studies that included 753 mechanically ventilated patients with shock (128). Eleven studies calculated the percent IVC diameter change (ΔIVC) as $[(IVC_{MAX} - IVC_{MIN})/IVC_{MIN}] \times 100$; one study used $[(IVC_{MAX} - IVC_{MIN})/[(IVC_{MAX} + IVC_{MIN})/2]] \times 100$. All studies defined volume responsiveness as an increase in stroke volume, cardiac output, or a surrogate measurement of at least 15% following a fluid bolus. The median ΔIVC threshold was 16%, and pooled sensitivity and specificity in patients receiving V_T greater than 8 mL/kg and PEEP less than or equal to 5 cmH_2O were 0.80 and 0.94, respectively (128).

Limitations

Although experimental evidence is lacking for many, several factors have been shown or predicted to significantly reduce the accuracy of SPV, PPV, SVV, and ΔIVC during mechanical ventilation (128, 138, 144). These limitations can be explained by the physiological principles underlying respiratory-cardiovascular interactions.

- *Low* V_T and *spontaneous inspiratory efforts* reduce the rise in P_{PL} and the fall in ventricular preload, thereby increasing the number of false-negative results. Studies have shown that mechanical breaths must be passive, and a V_T of at least 8 mL/kg is needed for acceptable accuracy (29, 128). Because most patients now receive volumes less than 8 mL/kg, a temporary increase in V_T is usually required during these measurements.

- At a given V_T, *low chest wall compliance* increases the rise in P_{PL} and the fall in ventricular preload during positive-pressure inflation (Figure 18B) (20, 61, 91, 96). This increases the number of false-positive results.
- *Intra-abdominal hypertension* decreases chest wall compliance, thereby exaggerating the fall in ventricular preload during mechanical inflation (91). Intra-abdominal hypertension also predisposes to a vascular waterfall, which makes P_{AB}, not $P_{RA\text{-}IM}$, the back pressure for lower body venous return (134, 135). Thus, SPV, PPV, SVV, and ΔIVC may be uncoupled from the change in P_{PL} and the response to volume infusion (10, 34, 79).
- In patients with *RV failure*, the reduction in RV preload during positive-pressure inflation may, through ventricular interaction, increase LV preload and stroke volume (92). On the other hand, the inflation-induced rise in RV afterload may reduce ventricular stroke volume. Either way, SPV, PPV, and SVV are unlikely to accurately predict the response to volume infusion. Right ventricular pressure and volume overload dilate the IVC; thus, ΔIVC is likely to be small even in volume-responsive patients.
- An *irregular cardiac rhythm* (e.g., atrial fibrillation) constantly changes ventricular preload through its effects on diastolic filling time independent of ventilation-induced variations. Thus, SPV, PPV, SVV, and ΔIVC are not useful in predicting the response to volume infusion.

Conclusion

Ventilation influences cardiovascular function by altering the extramural pressures acting on the heart and the intrathoracic and intra-abdominal blood vessels. The elevation in P_{ALV}, P_{PL}, $P_{L\text{-}TM}$, and P_{AB} produced by mechanical inflation and PEEP is accompanied by a reduction in RV and LV preload and LV afterload and an increase in RV afterload. The magnitude and clinical significance of the resulting hemodynamic effects depend on the delivered tidal volume, $PEEP_T$, lung and chest wall compliance, intravascular volume, intra-abdominal pressure, and baseline RV and LV function.

Related Articles

Aerodynamic Theory
Interactions Between Respiration and Circulation
Mechanical Interaction of Respiration and Circulation
Dynamics of Respiration
Pressure–Flow Relationships in the Lungs

References

1. Agostoni E, Hyatt RE. Static behavior of the respiratory system. *Compr Physiol*, 2011, Supplement 12: Handbook of Physiology, The Respiratory System, The Mechanics of Breathing: 113-130. First published in print 1986. DOI: 10.1002/cphy.cp030309.
2. Albert RK, Hubmayr R. The hemodynamic effects of prone positioning in patients with acute respiratory distress syndrome remain to be defined. *Am J Resp Crit Care Med* 189: 1567, 2014.
3. Alviar CL, Miller PE, McAreavey D, Katz JN, Lee B, Moriyama B, Soble J, van Diepen S, Solomon MA, Morrow DA, ACC Critical Care Cardiology Working Group. Positive pressure ventilation in the cardiac intensive care unit. *J Am Coll Cardiol* 72: 1532-1553, 2018.
4. Ansari BM, Zochios V, Falter F, Klein AA. Physiological controversies and methods used to determine fluid responsiveness: A qualitative systematic review. *Anaesthesia* 71: 94-105, 2016.
5. Ashbaugh DG, Bigelow DB, Petty TL, Levine BE. Acute respiratory distress in adults. *Lancet* 2 (7511): 319-323, 1967.
6. Backofen JE, Schauble JF. Hemodynamic changes with prone positioning during general anesthesia. *Anesth Analg* 64: 194, 1995.
7. Barbier C, Loubieres Y, Schmit C, Hayon J, Ricome J-L, Vieillard-Baron A. Respiratory changes in inferior vena cava diameter are helpful in predicting fluid responsiveness in ventilated septic patients. *Intensive Care Med* 30: 1740-1746, 2004.
8. Benjamin JJ, Murtagh PS, Proctor DF, Menkes HA, Permutt S. Pulmonary vascular interdependence in excised dog lobes. *J Appl Physiol* 37: 887-894, 1974.
9. Berbenetz N, Wang Y, Brown J, Godfrey C, Ahmad M, Vital FM, Lambiase P, Banerjee A, Bakhai A, Chong M. Non-invasive positive pressure ventilation (CPAP or bilevel NPPV) for cardiogenic pulmonary oedema. *Cochrane Database Syst Rev* 4: CD005351, 2019.
10. Beurton A, Teboul JL, Girotto V, Galarza L, Anguel N, Richard C, Monnet X. Intra-abdominal hypertension is responsible for false negatives to the passive leg raising test. *Crit Care Med* 47: e639-e647, 2019.
11. Bishop VS, Horwitz LD, Stone HL, Stegall HF, Engelken EJ. Left ventricular internal diameter and cardiac function in conscious dogs. *J Appl Physiol* 27: 619-623, 1967.
12. Bishop VS, Stone HL, Guyton AC. Cardiac function curves in conscious dogs. *Am J Phys* 207: 677-682, 1964.
13. Blanch L, Mancebo J, Perez M, Martinez M, Mas A, Betbese AJ, Joseph D, Ballus J, Lucangelo U, Bak E. Short-term effects of prone position in critically ill patients with acute respiratory distress syndrome. *Intensive Care Med* 23: 1033-1039, 1997.
14. Blix M. Die lange und die spanning des muskels. *Skandinav Arch f Physiol* 5: 173, 1895.
15. Boissier F, Katsahian S, Razazi K, Thille AW, Roche-Campo F, Leon R, Vivier E, Brochard L, Vieillard-Baron A, Brun-Buisson C, Mekontso Dessap A. Prevalence and prognosis of cor pulmonale during protective ventilation for acute respiratory distress syndrome. *Intensive Care Med* 39: 1725-1733, 2013.
16. Brower R, Wise RA, Hassapoyannes C, Bromberger-Barnea B, Permutt S. Effect of lung inflation on lung blood volume and pulmonary venous flow. *J Appl Physiol* 58: 954-963, 1985.
17. Buda A, Pinsky MR, Jugels NB, Daughters GT, Stinson EB, Alderman EL. Effect of intrathoracic pressure on left ventricular performance. *N Engl J Med* 301: 453-459, 1979.
18. Burton AC, Patel DJ. Effect on pulmonary vascular resistance of inflation of the rabbit lungs. *J Appl Physiol* 12: 239-246.
19. Butler J. The adaptation of the relaxed lungs and chest wall to changes in volume. *Clin Sci* 16: 421-433, 1957.
20. Chapin JC, Downs JB, Douglas ME, Murphy EJ, Ruiz BC. Lung expansion, airway pressure transmission, and positive end-expiratory pressure. *Arch Surg* 114: 1193-1197, 1979.
21. Chirinos JA, Segars P. Noninvasive evaluation of left ventricular afterload, Part 1: pressure and flow measurements and basic principles of wave conduction and reflection. *Hypertension* 56: 555-562, 2010.
22. Coz Yataco A, Aguinaga Meza M, Buch KP, Disselkamp MA. Hospital and intensive care unit management of decompensated pulmonary hypertension and right ventricular failure. *Heart Fail Rev* 21: 323-346, 2016.
23. Culver BH, Butler J. Mechanical influences on the pulmonary microcirculation. *Ann Rev Physiol* 42: 187-198, 1980.
24. D'Angelo E, Calderini E, Torri G, Robatto FM, Bono D, Milic-Emili J. Respiratory mechanics in anesthetized, paralyzed humans: Effects of flow, volume, and time. *J Appl Physiol* 67: 2556-2564, 1989.
25. D'Angelo E, Prandi E, Tavola M, Calderini E, Milic-Emili J. Chest wall interrupter resistance in anesthetized, paralyzed humans. *J Appl Physiol* 77: 883-887, 1994.
26. D'Angelo E, Robatto FM, Calderini E, Tavola M, Bono D, Torri G, Milic-Emili J. Pulmonary and chest wall mechanics in anesthetized paralyzed humans. *J Appl Physiol* 70: 2602-2610, 1991.
27. Dalabih M, Rischard F, Mosier JM. What's new: The management of right ventricular decompensation of chronic pulmonary hypertension. *Intensive Care Med* 40: 1930-1933, 2014.
28. Dawson CA, Grimm DJ, Linehan JH. Effects of lung inflation on longitudinal distribution of pulmonary vascular resistance. *J Appl Physiol* 43: 1089-1092, 1977.
29. De Backer D, Heenen S, Piagnerelli M, Koch M, Vincent JL. Pulse pressure variations to predict fluid responsiveness: Influence of tidal volume. *Intensive Care Med* 31: 517-523, 2005.

30. De Troyer A, Loring SH. Action of the respiratory muscles. *Compr Physiol*, 2011, Supplement 12: Handbook of Physiology, The Respiratory System, The Mechanics of Breathing: 443-461. First published in print 1986. DOI: 10.1002/cphy.cp030326.
31. Dell'Italia LJ. Anatomy and physiology of the right ventricle. *Cardiol Clin* 30: 167-187, 2012.
32. DeTroyer A, Wilson TA. Action of the diaphragm on the rib cage. *J Appl Physiol* 121: 391-400, 2016.
33. Ducros L, Logeart D, Vicaut E, Henry P, Plaisance P, Collet JP, Broche C, Gueye P, Vergne M, Goetgheber D, Pennec PY, Belpomme V, Tartiere JM, Lagarde S, Placente M, Fievet ML, Montalescot G, Payen D. CPAP for acute cardiogenic pulmonary oedema from out-of-hospital to cardiac intensive care unit: A randomized, multicentre study. *Intensive Care Med* 37: 1501-1509, 2011.
34. Duperret S, Lhuillier F, Piriou V. Increased intra-abdominal pressure affects respiratory variations in arterial pressure in normovolaemic and hypovolaemic mechanically ventilated healthy pigs. *Intensive Care Med* 33: 163-171, 2007.
35. Feihl F, Broccard AF. Interactions between respiration and systemic hemodynamics. Part I: Basic concepts. *Intensive Care Med* 35: 45-54, 2009.
36. Fessler HE. Heart-lung interactions: Applications in the critically ill. *Eur Resp J* 10: 226-237, 1997.
37. Fessler HE, Brower RG, Shapiro EP, Permutt S. Effects of positive end-expiratory pressure and body position on pressure in the thoracic great veins. *Am Rev Respir Dis* 148: 1657-1664, 1993.
38. Fessler HE, Brower RG, Wise RA, Permutt S. Mechanism of reduced LV afterload by systolic and diastolic positive pleural pressure. *J Appl Physiol* 65: 1244-1250, 1988.
39. Fessler HE, Brower RG, Wise RA, Permutt S. Effects of positive end-expiratory pressure on the gradient for venous return. *Am Rev Respir Dis* 143: 19-24, 1991.
40. Fessler HE, Brower RG, Wise RA, Permutt S. Effects of positive end-expiratory pressure on the canine venous return curve. *Am Rev Respir Dis* 146: 4-10, 1992.
41. Fishman AP. Pulmonary circulation. *Compr Physiol*, 2011, Supplement 10: Handbook of Physiology, The Respiratory System, Circulation and Non-respiratory Functions: 1193-165. First published in print 1985. DOI: 10.1002/cphy.cp030103.
42. Frank O. For the dynamics of the heart muscle. *Z Biol* 32: 370-437, 1895.
43. Gattinoni L, Pelosi P, Suter PM, Pedoto A, Vercesi P, Lissoni A. Acute respiratory distress syndrome caused by pulmonary and extrapulmonary disease - different syndromes? *Am J Respir Crit Care Med* 158: 3-11, 1998.
44. Goshy M, Lai-Fook SJ, Hyatt RE. Perivascular pressure measurement by wick-catheter technique in isolated dog lobes. *J Appl Physiol* 46: 950-955, 1979.
45. Gray A, Goodacre S, Newby DE, Masson M, Sampson F, Nicholl J. Noninvasive ventilation in acute cardiogenic pulmonary edema. *N Engl J Med* 359: 142-151, 2008.
46. Guérin C, Reignier J, Richard JC, Beuret P, Gacouin A, Boulain T, Mercier E, Badet M, Mercat A, Baudin O, Clavel M, Chatellier D, Jaber S, Rosselli S, Mancebo J, Sirodot M, Hilbert G, Bengler C, Richecoeur J, Gainnier M, Bayle F, Bourdin G, Leray V, Girard R, Baboi L, Ayzac L. Prone positioning in severe acute respiratory distress syndrome. *N Engl J Med* 368: 2159-2168, 2013.
47. Guyton AC. Determination of cardiac output by equating venous return curves with cardiac response curves. *Physiol Rev* 35: 123-129, 1955.
48. Guyton AC, Abernathy B, Langston JB, Kaufmann BN, Fairchild HM. Relative importance of venous and arterial resistances in controlling venous return and cardiac output. *Am J Phys* 196: 1008-1014, 1959.
49. Guyton AC, Armstrong GG, Chipley PL. Pressure-volume curves of the of the arterial and venous systems in live dogs. *Am J Phys* 184: 253-258, 1956.
50. Guyton AC, Lindsey AW, Abernathy B, Richardson T. Venous return at various right atrial pressures and the normal venous return curve. *Am J Phys* 189: 609-615, 1957.
51. Guyton AC, Polizo D, Armstrong GG. Mean circulatory filling pressure immediately after cessation of heart pumping. *Am J Phys* 179: 261-267, 1954.
52. Hakim TS, Michel RP, Chang HK. Effect of lung inflation on pulmonary vascular resistance by arterial and venous occlusion. *J Appl Physiol* 53: 1110-1115, 1982.
53. Hering R, Wrigge H, Vorwerk R, Brensing KA, Schroder S, Zinserling J, Hoeft A, Spiegel TV, Putensen C. The effects of prone positioning on intraabdominal pressure and cardiovascular and renal function in patients with acute lung injury. *Anesth Analg* 92: 1226-1231, 2001.
54. Hibberd MG, Jewell BR. Calcium- and length- dependent force production in rat ventricular muscle. *J Physiol* 329: 527-540, 1982.
55. Hoeper MM, Granton J. Intensive care unit management of patients with severe pulmonary hypertension and right heart failure. *Am J Resp Crit Care Med* 184: 1114-1124, 2011.
56. Howell JBL, Permutt S, Proctor DF, Riley RL. Effect of inflation of the lung on different parts of the pulmonary vascular bed. *J Appl Physiol* 16: 71-76, 1961.
57. Ingram RH, Pedley TJ. Pressure-flow relationships in the lungs. *Compr Physiol*, 2011, Supplement 12: Handbook of Physiology, The Respiratory System, The Mechanics of Breathing: 277-293. First published in print 1986. DOI: 10.1002/cphy.cp030318.
58. Jardin F. Cyclic changes in arterial pressure during mechanical ventilation. *Intensive Care Med* 30: 1047-1050, 2004.
59. Jardin F, Delorme G, Hardy A, Auvert B, Beauchet A, Bourdarias JP. Reevaluation of hemodynamic consequences of positive pressure ventilation: Emphasis on cyclic right ventricular afterloading by mechanical lung inflation. *Anesthesiology* 72: 966-970, 1990.
60. Jardin F, Farcot JC, Boisante L, Prost JF, Guéret P, Bourdarias JP. Mechanism of paradoxical pulse in bronchial asthma. *Circulation* 66: 887-894, 1982.
61. Jardin F, Genevray B, Brun-Ney D, Bourdarias JP. Influence of lung and chest wall compliances on transmission of airway pressure to the pleural space in critically ill patients. *Chest* 88: 653-658, 1985.
62. Jardin F, Gueret P, Dubourg O. Two-dimensional echocardiographic evaluation of right ventricular size and contractility in acute respiratory failure. *Crit Care Med* 13: 952-956, 1985.
63. Jardin F, Vieillard-Baron A. Is there a safe plateau pressure in ARDS? The right heart only knows. *Intensive Care Med* 33: 444-447, 2007.
64. Jellinek H, Krenn H, Oczenski W, Veit F, Schwarz S, Fitzgerald RD. Influence of positive airway pressure on the pressure gradient for venous return in humans. *J Appl Physiol* 88: 926-932, 2000.
65. Jonson B, Laurent B, Brauer K, Mansson C, Valind S, Grytzell H. Mechanics of the respiratory system in healthy anesthetized humans with emphasis on viscoelastic properties. *J Appl Physiol* 75: 132-140, 1993.
66. Jozwiak M, Teboul J-L, Anguel N, Persichini R, Silva S, Chemla D, Richard C, Monnet X. Beneficial hemodynamic effects of prone positioning in patients with acute respiratory distress syndrome. *Am J Respir Crit Care Med* 188: 1428-1433, 2013.
67. Jubran A, Mathru M, Dries D, Tobin MJ. Continuous recordings of mixed venous oxygen saturation during weaning from mechanical ventilation and the ramifications thereof. *Am J Respir Crit Care Med* 158: 1763-1769, 1998.
68. Kerbaul F, Rondelet B, Motte S, Fesler P, Hubloue I, Ewalenko P, Naeije R, Brimioulle S. Effects of norepinephrine and dobutamine on pressure load-induced right ventricular failure. *Crit Care Med* 32: 1035-1040, 2004.
69. Krishnam S, Schmidt GA. Acute right ventricular dysfunction: Real-time management with echocardiography. *Chest* 147: 835-846, 2015.
70. Kuramoto K, Rodbard S. Ventilation effects on left atrium and pulmonary vascular resistance. *J Appl Physiol* 18: 117-122, 1963.
71. Lakatta EG, Jewell BR. Length-dependent activation: Its effect on the length-tension relation in cat ventricular muscle. *Circ Res* 40: 251-257, 1977.
72. Lansdorp B, Hofhuizen C, van Lavieren M, van Swieten H, Lemson J, van Putten M, van der Hoeven JG, Pickkers P. Mechanical ventilation-induced intrathoracic pressure distribution and heart-lung interactions. *Crit Care Med* 42: 1983-1990, 2014.
73. Lemaire F, Teboul JL, Cinotti L, Giotto G, Abrouk F, Steg G, Macquin-Mavier I, Zapol WM. Acute left ventricular dysfunction during unsuccessful weaning from mechanical ventilation. *Anesthesiology* 69: 171-179, 1988.
74. Lheritier G, Legras A, Caille A, Lherm T, Mathonnet A, Frat JP, Courte A, Martin-Lefevre L, Gouello JP, Amiel JB, Garot D, Vignon P. Prevalence and prognostic value of acute cor pulmonale and patent foramen ovale in ventilated patients with early acute respiratory distress syndrome: A multicenter study. *Intensive Care Med* 39: 1734-1742, 2013.
75. Lumb AB. *Nunn's Applied Respiratory Physiology*. Edinburgh: Elsevier, 2010.
76. Maas JJ, de Wilde RB, Aarts LP, Pinsky MR, Jansen JR. Determination of vascular waterfall phenomenon by bedside measurement of mean systemic filling pressure and critical closing pressure in the intensive care unit. *Anesth Analg* 114: 803-810, 2012.
77. Magder S. Is all on the level? Hemodynamics during supine versus prone ventilation. *Am J Resp Crit Care Med* 188: 1390-1391, 2013.
78. Magder S. Heart-lung interaction in spontaneously breathing subjects: The basics. *Ann Transl Med* 6: 348, 2018. DOI: 10.21037/atm.2018.06.19.
79. Mahjoub Y, Touzeau J, Airapetian N, Lorne E, Hijazi M, Zogheib E, Tinturier F, Slama M, Dupont H. The passive leg-raising maneuver cannot accurately predict fluid responsiveness in patients with intra-abdominal hypertension. *Crit Care Med* 38: 1824-1829, 2010.
80. Marik PE, Cavallazzi R. Does the central venous pressure predict fluid responsiveness? An updated meta-analysis and a plea for some common sense. *Crit Care Med* 41: 1774-1781, 2013.
81. Marik PE, Cavallazzi R, Vasu T, Hirani A. Dynamic changes in arterial waveform derived variables and fluid responsiveness in mechanically

ventilated patients: A systematic review of the literature. *Crit Care Med* 37: 2642-2647, 2009.
82. Marini JJ. Dynamic hyperinflation and auto-positive end-expiratory pressure. *Am J Respir Crit Care Med* 184: 756-762, 2011.
83. Markwalder J, Starling EH. On the constancy of the systolic output under varying conditions. *J Physiol* 48: 348-356, 1914.
84. Masip J, Betbesé AJ, Páez J, Vecilla F, Canizares R, Padro J, Paz MA, de Otero J, Ballus J. Non-invasive pressure support ventilation versus conventional oxygen therapy in acute cardiogenic pulmonary oedema: A randomised trial. *Lancet* 356: 2126-2132, 2000.
85. Mead J. Mechanical properties of lungs. *Physiol Rev* 41: 281-329, 1961.
86. Mead J, Whittenberger JL. Physical properties of human lungs measured during spontaneous respiration. *J Appl Physiol* 5: 779-796, 1953.
87. Mead J, Whittenberger L, Radford EP. Surface tension as a factor in pulmonary volume-pressure hysteresis. *J Appl Physiol* 10: 191-196, 1957.
88. Mekontso Dessap A, Boissier F, Charron C, Begot E, Repesse X, Legras A, Brun-Buisson C, Vignon P, Vieillard-Baron A. Acute cor pulmonale during protective ventilation for acute respiratory distress syndrome: Prevalence, predictors, and clinical impact. *Intensive Care Med* 42: 862-870, 2016.
89. Mekontso Dessap A, Charron C, Devaquet J, Aboab J, Jardin F, Brochard L, Vieillard-Baron A. Impact of acute hypercapnia and augmented positive end-expiratory pressure on right ventricle function in severe acute respiratory distress syndrome. *Intensive Care Med* 35: 1850-1858, 2009.
90. Mentzelopoulos SD, Roussos C, Zakynthinos SG. Static pressure volume curves and body posture in acute respiratory failure. *Intensive Care Med* 31: 1683-1692, 2005.
91. Mesquida J, Kim HK, Pinsky MR. Effect of tidal volume, intrathoracic pressure, and cardiac contractility on variations in pulse pressure, stroke volume, and intrathoracic blood volume. *Intensive Care Med* 37: 1672-1679, 2011.
92. Naeije R, Badagliacca R. The overloaded right heart and ventricular interdependence. *Cardiovasc Res* 113: 1474-1485, 2017.
93. Naeije R, Brimioulle S, Dewachter L. Biomechanics of the right ventricle in health and disease. *Pulm Circ* 4: 395-406, 2014.
94. Nanas S, Magder S. Adaptations of the peripheral circulation to PEEP. *Am Rev Respir Dis* 146: 688-693, 1992.
95. Nava S, Carbone G, DiBattista N, Bellone A, Baiardi P, Cosentini R, Marenco M, Giostra F, Borasi G, Groff P. Noninvasive ventilation in cardiogenic pulmonary edema: A multicenter randomized trial. *Am J Respir Crit Care Med* 168: 1432-1433, 2003.
96. O'Quinn RJ, Marini JJ, Culver BH, Butler J. Transmission of airway pressure to pleural space during lung edema and chest wall restriction. *J Appl Physiol* 59: 1171-1177, 1985.
97. Osman D, Monnet X, Castelain V, Anguel N, Warszawski J, Teboul JL. Incidence and prognostic value of right ventricular failure in acute respiratory distress syndrome. *Intensive Care Med* 35: 69-76, 2009.
98. Otis AB, Fenn WO, Rahn H. Mechanics of breathing in man. *J Appl Physiol* 2: 592-607, 1950.
99. Park M, Sangean MC, Volpe Mde S, Feltrim M, Nozawa E, Leite PF, Passos Amato MB, Lorenzi-Filho G. Randomized, prospective trial of oxygen, continuous positive airway pressure, and bilevel positive airway pressure by face mask in acute cardiogenic pulmonary edema. *Crit Care Med* 32: 2407-2415, 2004.
100. Paternot A, Repesse X, Vieillard-Baron A. Rationale and description of right ventricle-protective ventilation in ARDS. *Respir Care* 61: 1391-1396, 2016.
101. Patterson SW, Piper H, Starling EH. The regulation of the heartbeat. *J Physiol* 48: 465-513, 1914.
102. Patterson SW, Starling EH. On the mechanical factors which determine the output of the ventricles. *J Physiol* 48 (5): 357-379, 1914.
103. Pelosi P, Cereda M, Foti G, Giacomini M, Pesenti A. Alterations of lung and chest wall mechanics in patients with acute lung injury: Effects of end-expiratory pressure. *Am J Resp Crit Care Med* 152: 531-537, 1995.
104. Pelosi P, Tubiolo D, Mascheroni D, Vicardi P, Crotti S, Valenza F, Gattinoni L. Effects of the prone position on respiratory mechanics and gas exchange during acute lung injury. *Am J Respir Crit Care Med* 157: 387-393, 1998.
105. Perel A. The physiological basis of arterial pressure variation during positive-pressure ventilation. *Reanimation* 14: 162-171, 2005.
106. Perel A, Pizov R, Cotev S. Systolic blood pressure variation is a sensitive indicator of hypovolemia in ventilated dogs subjected to graded hemorrhage. *Anesthesiology* 67: 498-502, 1987.
107. Permutt S, Howell JBL, Proctor DF, Riley RL. Effect of lung inflation on static pressure-volume characteristics of pulmonary vessels. *J Appl Physiol* 16: 64-70, 1961.
108. Permutt S, Martin HB. Static pressure-volume characteristics of lungs in normal males. *J Appl Physiol* 15: 819-825, 1960.
109. Permutt S, Riley RL. Hemodynamics of collapsible vessels with tone: The vascular waterfall. *J Appl Physiol* 18: 924-932, 1963.
110. Petak F, Albu G, Lele E, Morel DR, Fontao F, Habre W. Lung mechanical and vascular changes during positive- and negative-pressure lung inflations: Importance of reference pressures in the pulmonary vasculature. *J Appl Physiol* 106: 935-942, 2009.
111. Pinsky M. Instantaneous venous return curves in an intact canine preparation. *J Appl Physiol* 56: 765-771, 1984.
112. Pinsky MR. Determinants of pulmonary arterial flow variation during respiration. *J Appl Physiol* 56: 1237-1245, 1984.
113. Pinsky MR, Matuschak GM, Klain M. Determinants of cardiac augmentation by elevations in intrathoracic pressure. *J Appl Physiol* 58: 1189-1198, 1985.
114. Pinsky MR, Summer WR, Wise RA, Permutt S, Bromberger-Barnea B. Augmentation of cardiac function by elevation of intrathoracic pressure. *J Appl Physiol* 54: 950-955, 1983.
115. Purmutt S, Wise RA. Mechanical interaction of respiration and circulation. *Compr Physiol*, 2011, Supplement 12: Handbook of Physiology, The Respiratory System, The Mechanics of Breathing: 647-656. First published in print 1986. DOI: 10.1002/cphy.cp030336.
116. Rahn H, Otis AB, Chadwick LE, Fenn WO. The pressure-volume diagram of the thorax and lung. *Am J Phys* 146: 161-178, 1946.
117. Ranieri VM, Brienza N, Santostasi S, Puntillo F, Mascia L, Vitale N, Giuliani R, Memeo V, Bruno F, Fiore T, Brienza A, Stutsky AS. Impairment of lung and chest wall mechanics in patients with acute respiratory distress syndrome. *Am J Respir Crit Care Med* 156: 1082-1091, 1997.
118. Repessé X, Charron C, Guillaume G, Aubry A, Paternot A, Maizel J, Slama M, Vieillard-Baron A. Impact of positive pressure ventilation on mean systemic filling pressure in critically ill patients after death. *J Appl Physiol* 122: 1373-1378, 2017.
119. Rodarte JR, Rehder K. Dynamics of respiration. *Compr Physiol*, 2011, Supplement 12: Handbook of Physiology, The Respiratory System, The Mechanics of Breathing: 131-144. First published in print 1986. DOI: 10.1002/cphy.cp030310.
120. Roos A, Thomas LJ, Nagel EL, Prommas DC. Pulmonary vascular resistance as determined by lung inflation and vascular pressures. *J Appl Physiol* 16: 77-84, 1961.
121. Sanz J, Sanchez-Quintana D, Bossone E, Bogaard HJ, Naeije R. Anatomy, function, and dysfunction of the right ventricle. *J Am Coll Cardiol* 73: 1463-1482, 2019.
122. Sarnoff SJ. Myocardial contractility as described by ventricular function curves: Observations on Starling's law of the heart. *Physiol Rev* 35: 107-122, 1955.
123. Saugel B, Thiele RH, Hapfelmeier A, Cannesson M. Technological assessment and objective evaluation of minimally invasive and noninvasive cardiac output monitoring systems. *Anesthesiology* 133: 921-928, 2020.
124. Savale L, Weatherald J, Jaïs X, Vuillard C, Boucly A, Jevnikar M, Montani D, Mercier O, Simonneau G, Fadel E, Sitbon O, Humbert M. Acute decompensated pulmonary hypertension. *Eur Respir Rev* 26, 2017. DOI: 10.1183/16000617.
125. Schmitt JM, Vieillard-Baron A, Augarde R, Prin S, Page B, Jardin F. Positive end-expiratory pressure titration in acute respiratory distress syndrome patients: Impact on right ventricular outflow impedance evaluated by pulmonary artery Doppler flow velocity measurements. *Crit Care Med* 29: 1154-1158, 2001.
126. Sharp JT, Johnson FN, Goldberg NB, Van Lith P. Hysteresis and stress adaptation in the human respiratory system. *J Appl Physiol* 23: 487-497, 1967.
127. Shi R, Monnet X, Teboul JL. Parameters of fluid responsiveness. *Curr Opin Crit Care* 26: 319-326, 2020.
128. Si X, Xu H, Liu Z. Does respiratory variation in inferior vena cava diameter predict fluid responsiveness in mechanically ventilated patients? A systematic review and meta-analysis. *Anesth Analg* 127: 1157-1164, 2018.
129. Simmons D, Linde L, Miller J, O'Reilly R. Relation between lung volume and pulmonary vascular resistance. *Circ Res* 9: 465-471, 1961.
130. Slutsky AS, Ranieri VM. Ventilator-induced lung injury. *N Engl J Med* 369: 2126-2136, 2013.
131. Smith JC, Mitzner W. Analysis of pulmonary vascular interdependence in excised dog lobes. *J Appl Physiol* 48: 450-467, 1980.
132. Spinale FG. Assessment of cardiac function – basic principles and approaches. *Compr Physiol* 5: 1911-1946, 2015.
133. Spotnitz HM, Sonnenblick EH, Spiro D. Relation of ultrastructure to function in the intact heart: Sarcomere structure relative to pressure volume curves of intact left ventricles of dog and cat. *Circ Res* 18: 49-66, 1966.
134. Takata M, Robotham JL. Effects of abdominal pressure on venous return: Abdominal vascular zone conditions. *J Appl Physiol* 69: 1961-1972, 1990.
135. Takata M, Wise RA, Robotham JL. Effects of diaphragmatic inspiratory descent on inferior vena caval venous return. *J Appl Physiol* 72: 597-607, 1992.
136. Tanai E, Frantz S. Pathophysiology of heart failure. *Compr Physiol* 6: 187-214, 2016.
137. Taylor RR, Covell JW, Sonnenblick EH, Ross J. Dependence of ventricular distensibility on filling of the opposite ventricle. *Am J Phys* 213: 711-718, 1967.

138. Teboul JL, Monnet X, Chemla D, Michard F. Arterial pulse pressure variation with mechanical ventilation. *Am J Resp Crit Care Med* 199: 22-31, 2019.
139. Tedford RJ. Determinants of right ventricular afterload. *Pulm Circ* 4: 211-219, 2014.
140. Thomas LJ, Griffo ZJ, Roos A. Effect of negative-pressure inflation of the lung on pulmonary vascular resistance. *J Appl Physiol* 16: 451-456, 1961.
141. Toyota S, Amaki Y. Hemodynamic evaluation of the prone position by transesophageal echocardiography. *J Clin Anesth* 10: 32-35, 1998.
142. Van den Berg PCM, Jansen JRC, Pinsky MR. Effect of positive pressure on venous return in volume-loaded cardiac surgical patients. *J Appl Physiol* 92: 1223-1231, 2002.
143. Ventetuolo CE, Klinger JR. Management of acute right ventricular failure in the intensive care unit. *Ann Am Thorac Soc* 11: 811-822, 2014.
144. Via G, Tavazzi G, Price S. Ten situations where inferior vena cava ultrasound may fail to accurately predict fluid responsiveness: A physiologically based point of view. *Intensive Care Med* 42: 1164-1167, 2016.
145. Vieillard-Baron A, Augarde R, Prin S, Page B, Beauchet A, Jardin F. Influence of superior vena caval zone conditions on cyclic changes in right ventricular outflow during respiratory support. *Anesthesiology* 95: 1083-1088, 2001.
146. Vieillard-Baron A, Charron C, Caille V, Belliard G, Page B, Jardin F. Prone positioning unloads the right ventricle in severe ARDS. *Chest* 132: 1440-1446, 2007.
147. Vieillard-Baron A, Chergui K, Rabiller A, Peyrouset O, Page B, Beauchet A, Jardin F. Superior vena caval collapsibility as a gauge of volume status in ventilated septic patients. *Intensive Care Med* 30: 1734-1739, 2004.
148. Vieillard-Baron A, Evrard B, Repesse X. Limited value of end-expiratory inferior vena cava diameter to predict fluid responsiveness and impact of intra-abdominal pressure. *Intensive Care Med* 44: 197-203, 2018.
149. Vieillard-Baron A, Loubieres Y, Schmitt JM, Page B, Dubourg O, Jardin F. Cyclic changes in right ventricular output impedance during mechanical ventilation. *J Appl Physiol* 87: 1644-1670, 1999.
150. Vieillard-Baron A, Price LC, Matthay MA. Acute cor pulmonale in ARDS. *Intensive Care Med* 39: 1836-1838, 2013.
151. Vieillard-Baron A, Schmitt JM, Augarde R, Fellahi JL, Prin S, Page B, Beauchet A, Jardin F. Acute cor pulmonale in acute respiratory distress syndrome submitted to protective ventilation: Incidence, clinical implications, and prognosis. *Crit Care Med* 29: 1551-1555, 2001.
152. Villar J, Blazquez MA, Lubillo S, Quintana J, Manzano JL. Pulmonary hypertension in acute respiratory failure. *Crit Care Med* 17: 523-526, 1989.
153. Vonk-Noordegraff A, Chin KM, Haddad F, Hassoun PM, Hemnes AR, Hopkins SR, Kawut SM, Langleben D, Lumens J, Naeije R. Pathophysiology of the right ventricle and of the pulmonary circulation in pulmonary hypertension: An update. *Eur Resp J* 53, 2019. DOI: 10.1183/13993003.01900-2018.
154. Vonk-Noordegraff A, Westerhof BE, Westerhof N. The relationship between the right ventricle and its load in pulmonary hypertension. *J Am Coll Cardiol* 69: 236-243, 2017.
155. Voorhees AP, Han H-C. Biomechanics of cardiac function. *Compr Physiol* 5: 1623-1644, 2015.
156. Weng CL, Zhao YT, Liu QH, Fu CF, Sun F, Ma YL, Chen YW, He QY. Meta-analysis: Noninvasive ventilation in acute cardiogenic pulmonary edema. *Ann Intern Med* 152: 590-600, 2010.
157. West JB, Dollery CT, Naimark A. Distribution of blood flow in isolated lung: Relation to vascular and alveolar pressures. *J Appl Physiol* 19: 713-724, 1964.
158. Whittenberger JL, McGregor M, Berglund E, Horst HG. Influence of state of inflation of the lung on pulmonary vascular resistance. *J Appl Physiol* 15: 878-882, 1960.
159. Wiedemann HP, Wheeler AP, Bernard GR. Comparison of two fluid-management strategies in acute lung injury. *N Engl J Med* 354: 2564-2575, 2006.
160. Williams L, Frenneaux M. Diastolic ventricular interaction: From physiology to clinical practice. *Nature Clin Pract Cardiovasc Med* 3: 368-376, 2006.
161. Wise RA, Robotham JL, Summer WR. Effects of spontaneous ventilation on the circulation. *Lung* 159: 175-186, 1981.
162. Yang X, Du B. Does pulse pressure variation predict fluid responsiveness in critically ill patients? A systematic review and meta-analysis. *Crit Care* 18: 650, 2014. DOI: 10.1186/s13054-014-0650-6.
163. Zapol W, Jones R. Vascular component of ARDS: Clinical pulmonary hemodynamics and morphology. *Am Rev Respir Dis* 136: 471-474, 1987.
164. Zapol W, Snider M. Pulmonary hypertension in acute severe respiratory failure. *N Engl J Med* 296: 476-480, 1977.